Fatigue behavior of concrete: A literature review on the main relevant parameters

Fatima Zahraa Kachkouch, Camila Carvalho Noberto, Lucas Feitosa de Albuquerque Lima Babadopulos, Abcael Ronald Santos Melo, Amanda Moreira Lima Machado, Nassim Sebaibi, Fouad Boukhelf, Yassine El Mendili

Fatigue behavior of concrete: a literature review on the main relevant parameters

Fatima Zahraa KACHKOUCH[1], Camila Carvalho NOBERTO[2], Lucas Feitosa de Albuquerque Lima BABADOPULOS[2], Abcael Ronald Santos MELO[3], Amanda Moreira Lima MACHADO[2], Nassim SEBAIBI[1], Fouad BOUKHELF[1], Yassine EL MENDILI[1*]

[1] École supérieure d'ingénieurs des travaux de la construction de Caen, 1 rue Pierre et Marie Curie, Epron 14610, France.

[2] Programa de Pós-Graduação em Engenharia Civil: Estruturas e Construção Civil (PEC), Departamento de Engenharia Estrutural e Construção Civil (DEECC), Centro de Tecnologia (CT), Universidade Federal do Ceará (UFC), Bloco 733, Campus do Pici s/n, CEP 60440-900, Fortaleza-CE, Brasil.

[3] Curso de Engenharia Civil da Universidade Federal do Ceará (UFC), Centro de Tecnologia (CT), Universidade Federal do Ceará (UFC), Bloco 733, Campus do Pici s/n, CEP 60440-900, Fortaleza-CE, Brasil.

*Corresponding author. Tel: +33 231 452 628. E-mail: yassine.el-mendili@esitc-caen.fr

Abstract

This paper contributes by summarizing knowledge on the fatigue behavior of concrete, discussing current standardization, and organizing previous contributions and prospecting future developments in experimental research. It describes classical laboratory fatigue tests and analysis (S-N curves, damage effects on modulus etc.), emphasizing differences expected for real loading (with variation in frequency and temperature, among other effects). Not only current standards diverge in results, but more fundamental effects were observed. Temperature has relevant impact on fatigue life, and during tests it may change due to self-heating. Specimen dimensions are relevant for this phenomenon. Loading frequency seems to influence fatigue, and since tests in laboratory need to be accelerated (high frequency) compared to the field (low frequency), this is a major concern. Other investigated effects include loading waveforms and moisture.

Keywords: Concrete, Dynamic loading, Fatigue, Design, Wind turbine foundations.

Nomenclature

Symbol	
σ_{max}	Maximum applied stress
σ_{min}	Minimum applied stress
S_{max}	Maximum applied stress level
S_{min}	Minimum applied stress level
σ_a	Average stress
σ_r	Range stress
N	Number of cycles in a test and/or loading
Nf	Number of cycles to failure
R	Stress ratio
fc_{28}	Concrete's compressive strength at 28 days after mixing
HSC	High Strength Concrete
DNV	Det Norske Veritas
NSC	Normal Strength Concrete
HSC	High-Strength concrete
LC	Lightweight Concrete
NC	Normal-weight Concrete
Cf	Parameter depending on the loading frequency
β	Parameter depending on the material
Df	Damage fraction
ε^{max}	Strain evolution
ε^{0}	Maximum strain
α, β and p	Coefficients to be recalibrated
ω	Fatigue damage function
$\dot{\varepsilon}^{+}$	Positive rate of the equivalent strain
ε^{p}	Plastic strain
ε^{vp}	Viscoplastic strain
$\varepsilon^{v,cum}$	Cumulative strain

I. Introduction

Many structures (roads, bridges, and wind turbines) could be exposed to phenomena resulting from the application of repeated cyclic loads [1] that induce a decrease in their performances with time. It has been shown that this type of load could be the reason for many structures' deteriorations [2–6] due to the microcracks formation in the cement matrix and its propagation within the material. The fatigue of a component is a phenomenon characterized by the deterioration that occurs due to the repetition of loads that individually cannot produce failure. It is associated with the microcracks and can also ultimately lead to failure through the coalescence of microcracks into macrocracks. The crack can be result of direct mechanical loads, temperature variations, and environmental changes (such as humidity). Such actions cause stresses within the material, which can produce long-term effects [7,8], and also eventually lead to failure. Slender structures such as wind turbines, whether onshore or offshore, are amongst the structures which are continuously subjected to cyclic loads and require concrete with specific characteristics [9–11]. Viswanath et al. [12] investigated fatigue testing on concrete cylindrical specimens for wind turbine foundations and emphasized the need for replacement of insufficient fatigue design recommendations for more accurate models. New recommendations should investigate the fatigue phenomenon further, considering more of the complexity of the concrete material's dynamic behavior.

The materials in such structures should support the existing repetitive and variable loads. Wind turbulence, vibrations, shocks, and explosions could impose dynamic forces close to the fundamental periods of the structure or its components with significant magnitude of loadings. Structures that respond to a given set of actions with resonant vibrations at one or more natural periods are evaluated by dynamic analysis techniques [13]. Earthquakes are also to be considered as oscillatory loads that require a dynamic analysis in the case where the studied area is part of a seismic zone that could cause important ground movements [14]. A classification of dynamic loads was given by Golewski [15] in his paper, according to their origins. The work also established a procedure of dynamic diagnostics of existing and forecast situations.

The applied cyclic loads should cover all the frequencies content likely to cause a relevant dynamic response in the structure. After many cycles (which could reach the order of magnitude of millions), the material gets in an irreversible damage phase, losing progressively its physical properties until failure. Such loadings are transmitted to the foundation, generating cracks in the concrete foundation, leading to fatigue with time. It is therefore essential to study the dynamic behavior of the concrete subjected to cyclic loads. The same can be said about concrete used in wind tower construction (including its foundation), i.e., fatigue is also a potential problem in such structures and should be assessed.

Research on concrete fatigue properties started at the end of the XIXth century [16,17]. Fig. 1 represents a timeline that illustrates the first relevant fatigue studies in compression, bending, and

tension. These investigations were performed before 1900 while contributions to fatigue were classified as historical. From 1900 to 1930, the first studies of fatigue behavior considered compression [18] and flexural tests [19,20]. Fatigue by tensile stress was not widely explored, at that time, because of the complexity of the test implementation. After 1930, Graf and Brenner [21] were the first authors who evaluated the effect of frequency on the dynamic behavior of concrete in compressive fatigue tests.

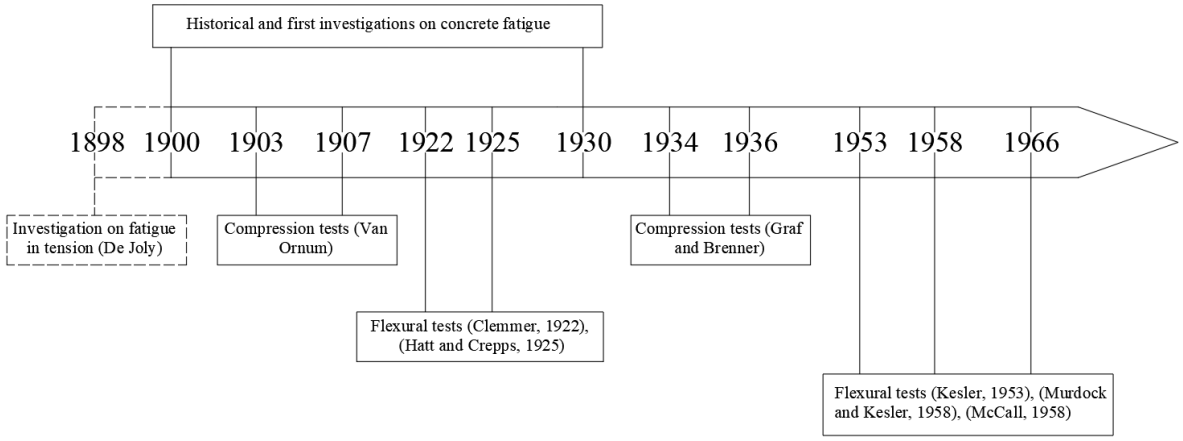

Fig. 1: Timeline of the history and first relevant studies of concrete fatigue. Timeline is continued in Section IV.1 (cf. Fig. 14).

In 1970, Aas-Jakobsen and Lenschow [22] developed a correlation relating the maximum applied stress level (S_{max}) with the number of cycles to failure (N*f*). Eq. (1) introduces the β factor (which depends on the material and is commonly considered equal to 0.0685) and the stress ratio ($R = S_{min}/S_{max}$) parameters.

$$S_{max} = 1 - \beta\,(1 - R)\,\log N_f \qquad (1)$$

This correlation was later modified by Tepfers and Kutti [23], considering the effect of loading frequency. In the same way, Furtak [24] proposed a new equation introducing a parameter C*f*, depending on the frequency in log scalse log*f*, equal to $C_f = 1 + a\,(1 - b.R)\,\log f$. A, B, C, a, and b are parameters depending on the material type. Such new equation is represented in Eq. (2).

$$S_{max} = CN^{-A}\,(1 + B \log Nf)\,C_f \qquad (2)$$

Due to the set of parameters that define equation (2), it seems complicated to manipulate it and to bring out the direct effect of the frequency. For that reason, an equation was developed directly from Eq. (1) by adding the coefficient C*f*, which permits to differentiate between S_{max} and fc_{28}, which leads to Eq. (3). According to the authors, the explanation for the direct introduction of C*f* in the basic equation was, that since S_{max} varies, the loading speed varies too, contrary to the effect of fc_{28}. This difference is therefore mainly due to the loading rate which corresponds to the frequency of the load application.

$$S_{max} = Cf\,[1 - \beta\,(1 - R)\log Nf] \qquad (3)$$

This is done as in other structures where fatigue studies had started previously, such as railways [25] for which the classical S-N curves, relating load levels to the fatigue life, were first proposed. Fatigue studies in many materials, including concrete, are being developed nowadays [5,26] and this is still a challenging topic, particularly for concrete structures classically designed using static loading information for the past 15 decades.

Relevant parameters to be considered while evaluating the fatigue strength for concrete are the concrete quality, the predominant loading effect (axial, bending, shear, bond, or appropriate combinations thereof), the stress state (pure compression, pure tension, or compression/tension), the surrounding environment (air, submerged) and the loading frequency. Many regulations are available worldwide, which are under continuous development since the 1970s, but discrepancies exist and literature indicates that concrete fatigue design needs further research and improved standardization [11].

II. Methodology

This paper aims at reuniting the body of knowledge on the mentioned relevant aspects of the dynamic behavior of concrete, focusing on the fatigue phenomenon, discussing their effects on current standardization, and organizing previous contributions from the literature to facilitate current research on wind turbine foundations concrete fatigue. The idea of this study derives from a Regional project in France, which includes a collaboration with Brazilian partners, both regions committed with the development of technology for renewable energy sources. This project deals with the dynamic behavior of wind turbine concrete foundations.

Following a review of the relevant existing literature, a conceptual framework has been illustrated in Fig. 2, which summarizes visually our research methodology. The working approach is divided into two main stages, each one composed of several steps. In the first step, a description of the fatigue behavior of concrete was given, containing the various standards and elements representing this phenomenon. The elements representing experimental investigations are also presented, followed by a brief description of numerical models used in the literature, notably the empirical and phenomenological ones, which were developed in order to better predict the damage and fatigue behavior of concrete, and specifying the advantages/limitations of each approach. Subsequently, the effect of influencing parameters on the fatigue failure of concrete was discussed. It should be noted that each parameter has its own degree of influence, and that all the parameters are closely related to each other, which complicates the understanding of the phenomena involved when studying fatigue. Finally, the lack of literature and the remaining issues to be addressed are presented in the conclusions and recommendations section, which will serve as basis for future experimental investigation.

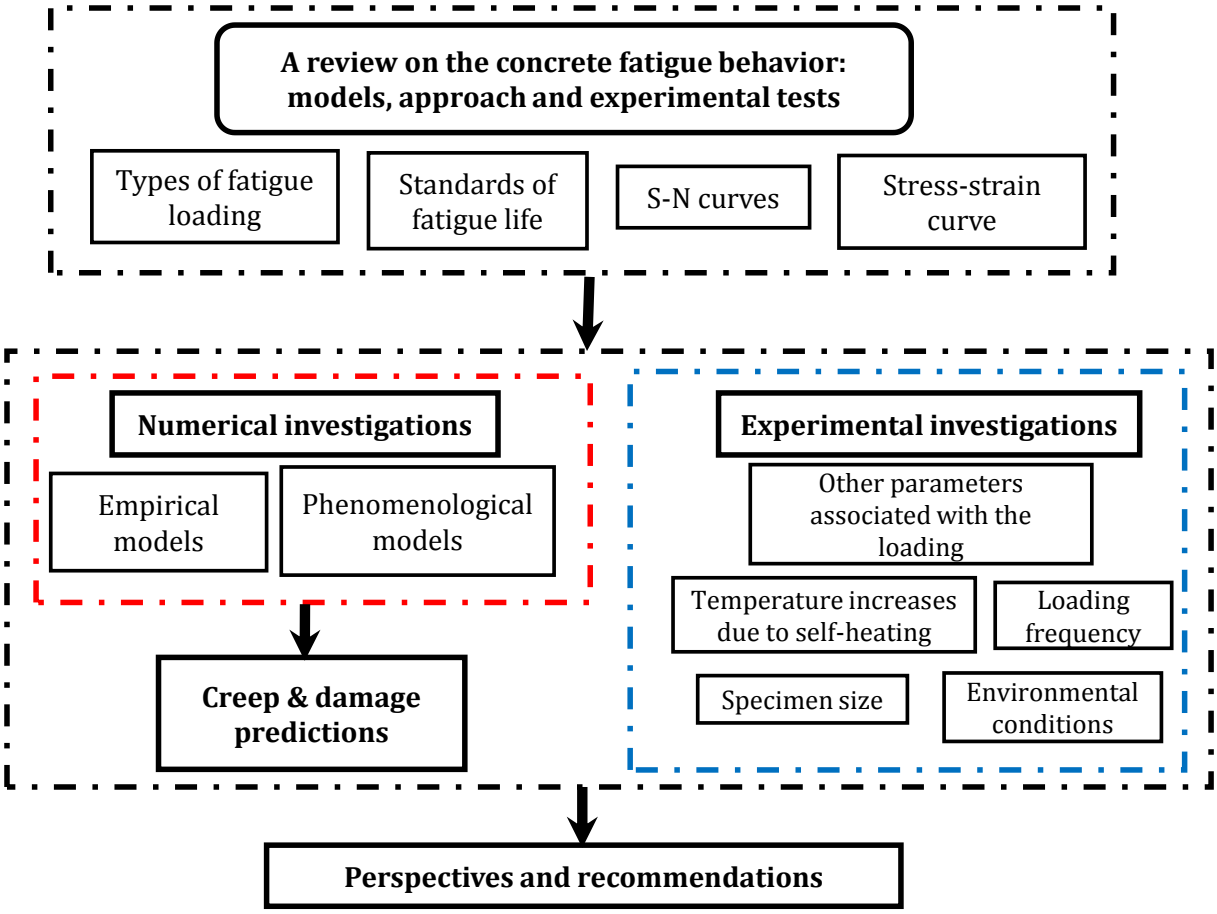

Fig.2: Summary of the research methodology in this paper as a schematic overview of the concrete fatigue behavior.

III. Fatigue behavior of concrete

III.1. Scientometric analysis

Given the importance of structural fatigue under external loading, a bibliometric analysis of literature is carried out. Several bibliometric properties of all the gathered papers were analyzed, with the aim of exposing the current state and evolution of knowledge surrounding the topics of fatigue behavior of concretes. Firstly, the keywords “concrete” and “fatigue" were analyzed on the Scopus database and the results were implemented in VOSviewer [27]. It is possible to see the origin countries of the first authors of 9135 papers, in relation with the other co-authors’ origin as shown in Fig. 3. This topic is widely studied in China, United states, Canada, United Kingdom, Australia, Germany, France, Brazil, Egypt, Japan, Netherlands, Portugal, among others. Indeed, three main contexts can be identified, specifically the study of the fatigue behavior of materials, in particular concrete, the properties characterization of new mixtures and experimental/numerical investigations of the mechanical behavior of structure elements constituted with/without reinforcement and subjected to compression/tension/bending loads as shown in Fig. 4, which displays main keywords on the same papers, which include: use of new materials (rubber, plastic recycling, graphite fibers etc.) and

composition studies; experimental (acoustic emission, bending, flexion, digital image correlation etc.) and numerical approaches (finite element method, stochastic models, Weibull distribution etc.); different applications (pavement design, bridge piers, wind power etc.); and different phenomena during tests (viscoelasticity, interfaces within materials, temperature effects etc.).

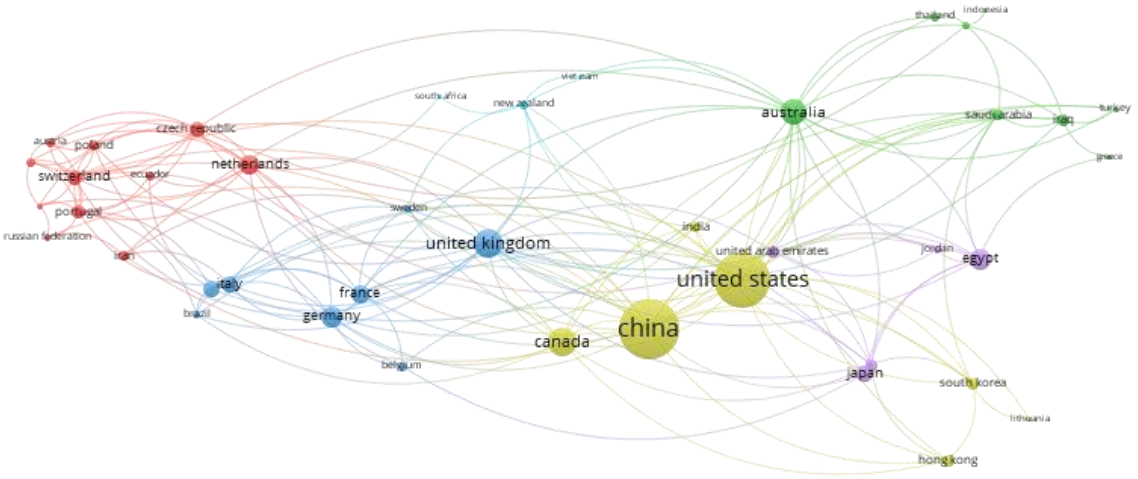

Fig. 3: Network of authors' and co-authors' origins of the articles on concrete fatigue in Scopus database.

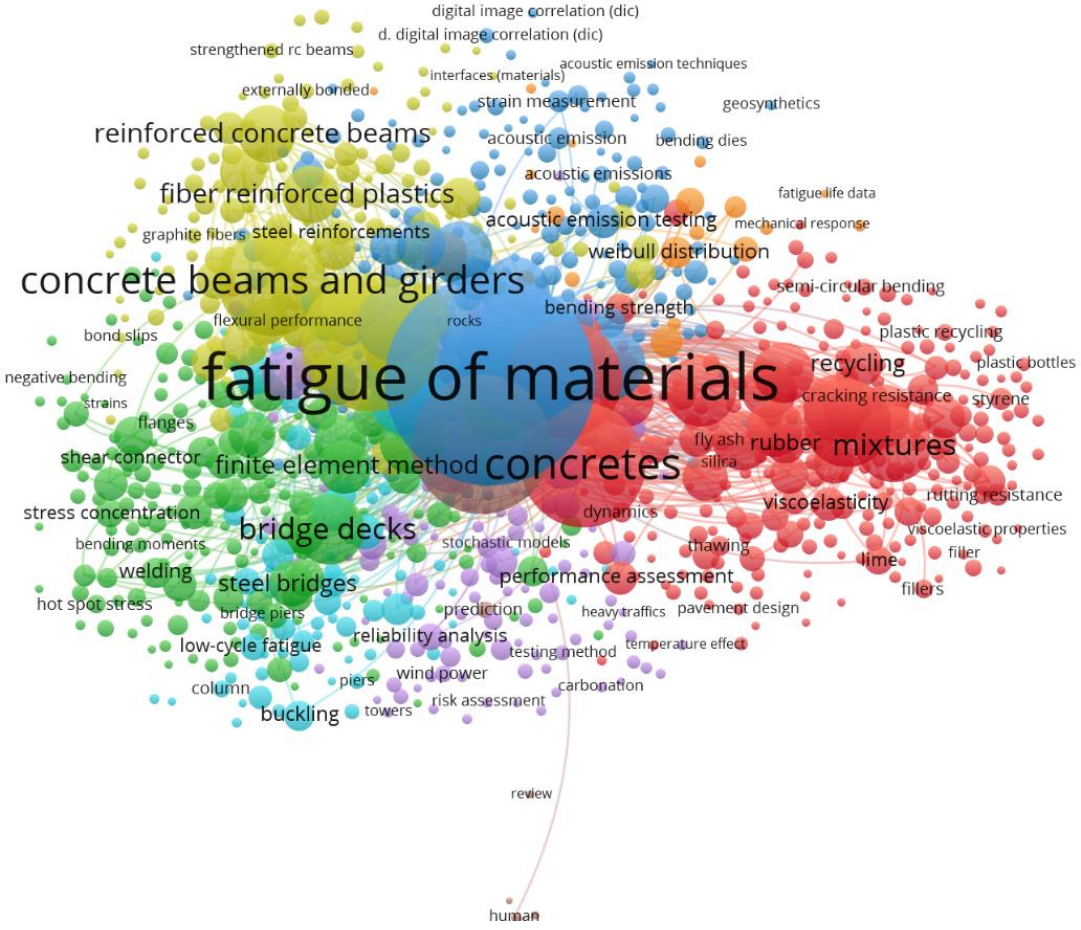

Fig. 4: Network of keywords of the articles on concrete fatigue in Scopus database.

III.2. Description of the physical phenomenon and standards used for fatigue tests

Two types of dynamic loading may exist on a structure: periodic loading or non-periodic loading. The first one is a repetitive loading that progresses repeated in the same way with time. It is also characterized by constant amplitude and a constant period and is either alternated (tension-compression, illustrated in Fig. 5a), or repeated (either with pure compression or pure tension, illustrated in Fig. 5a). Two types of periodic loads can be defined: (i) loads with a sinusoidal shape called a simple harmonic, and (ii) loads that are repetitive but have random shapes. These loads can be represented in the form of a mix of simple harmonics (such as in type 'i') using a Fourier analysis. Non-periodic loads, on the other hand, can be applied either as short-duration pulses or in long-duration but with arbitrary shapes. The first type of loading (type 'i') is the one most used in fatigue studies for characterization of the phenomenon, and it is believed to assess material properties in a way to represent best the loading behavior encountered in structures submitted to wind or traffic [28]. To apply this type of loading, it is necessary to know and understand some main parameters such as the maximum applied stress σ_{max}, which corresponds to the maximal stress to be applied in the test. It is usually chosen according to the strength of the material, normally a fraction of the strength (S_{max} and S_{min}). σ_{min} is the minimum stress to be applied, it could be defined by setting the stress ratio R. In the case of pure compression or pure tension Fig. 5b, this parameter has the same sign as σ_{max} (positive for tension and negative for compression). The average stress amplitude $\sigma_a = (\sigma_{max} - \sigma_{min})/2$ which, in most cases of experimental studies, is a main parameter used to perform the fatigue tests. The stress range $\sigma_r = (\sigma_{max} - \sigma_{min})$ is defined by the range in which the stress is applied. The maximum applied stress levels S_{max} and S_{min} are equal to σ_{max} / fc_{28} and σ_{min} / fc_{28}, respectively. Finally, the stress ratio $R = S_{min}/S_{max}$.

For fatigue experiments, servo-hydraulic testing machines apply repeated loads until failure. Figs. 5 (c,d) illustrates a cylindrical specimen of concrete before and after failure. As part of the ongoing collaborative project between French and Brazilian partners described previously, concrete is tested either under pure compression fatigue loading, using a hydraulic press with a loading capacity of 500 kN (as illustrated in Fig. 5), or in tension-compression using another hydraulic fatigue machine with smaller capacity.

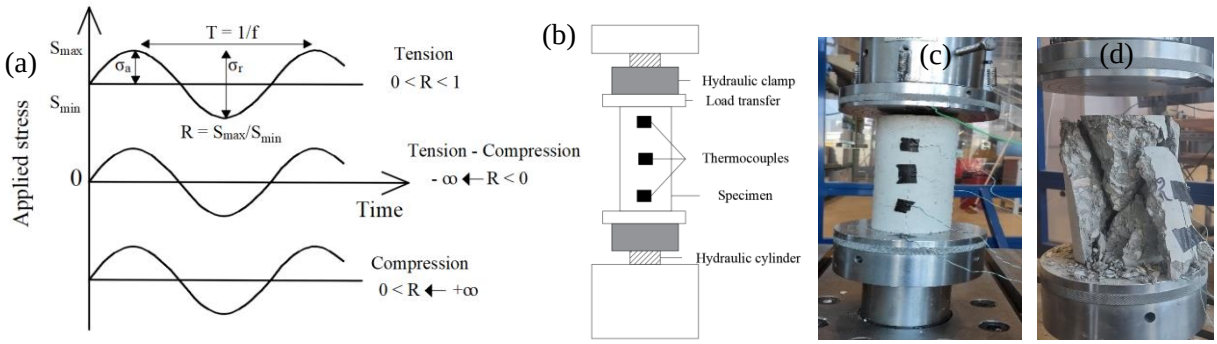

Fig. 5: (a) The applied periodic loadings of sinusoidal form called simple harmonic at various R-values. (b) A typical scheme for dynamic testing, applying pure compression to concrete samples, (c) before, and (d) after failure.

In real structures, the distribution of cyclic loads in time is typically random and is composed of a multitude of loads of non-regular amplitude. However, cyclic tests are generally carried out with cyclic loads with regular amplitude (periodic loads) and frequency maintained constant throughout the test. The transition from real to regular loading can be done by cycle counting methods derived from rainflow or cascade analyses [29–31]. Miner's damage accumulation concept (also known as Palmgreen-Miner's rule [32,33]) is then applied to determine accumulative damage due to cyclic stresses. It is evaluated by the calculation of the damage fraction Df (Eq. (4)). Df corresponds to the sum of the fatigue damage contributions for each stress range σ_r. It is obtained by calculating the sum over the many different loading conditions (i), for all stress ranges, of the ratio of the number of cycles expected at that condition (n_i) to the number of cycles required to produce failure (N_i). Fatigue occurs when the damage fraction reaches 100%, i.e., $D_f = 1$.

$$D_f = \sum_i \frac{n_i}{N_i} \qquad (4)$$

Several studies have focused on the dynamic behavior of wind turbine foundations [5,11,26]. Regulations try to cover the different requirements to establish structures resistant to the various applied stresses [34,35]. Among these regulations, there is the CEB-FIP model, which was first published in 1978, having as the latest model its version published in 2010. Also, the DNV-GL standard was published in 1974 and has many other versions [14,36]. These standards describe rules for the design of concrete structures, the different materials, and the dynamic behavior of concrete. Fatigue resistance equations have been established for this purpose and are used in the referred standards.

In Europe, the most used standard is the Model Code 2010 [37], in the USA the standard ACI PRC-215-92 [34] is the most common and the only one covering fatigue design of concrete in the USA. Nevertheless, it should be noted that there is no general code that specify several fields of application as a dynamic load of wind turbine foundations. In Brazil, although a national standard [38] proposes a

verification of fatigue for general structures, the focus is on the steel rebars' fatigue and not on the concrete itself. Then, for wind turbine foundations it is common to employ the European requirements. Wang and Fang [11] investigated different standards regarding concrete fatigue [10,34,35,37], by applying such codes to a common North-American wind turbine foundation (geometry and loads) and compared their results with finite element method and average sectional method results. The authors noted that the standards require different sets of analysis. For example, DNV-OS-H101 and Model Code 2010 [36,37] present requirements to shear cumulative fatigue damage. Wang and Fang [11] affirmed yet that the fatigue evaluation results can vary depending on the fatigue code employed. In addition, they said that several projects use European fatigue standards because of the availability of the most suppliers in Europe.

Golewski [39] presented some recommendations and requirements to implement, in an accurate way, Monolithic Pocket Foundations (PF) in order to resist to dynamic loads as well as static loads. A review containing guidelines for foundations for machines is also given by Golewski [40]. It gives recommendations for physical and mechanical properties of concrete constituting the foundation. The main purpose of the referred guidelines is to produce foundation which could be able not only to transfer loads but also to reduce vibrations produced by machines.

Børsheim [41] analyzed the fatigue loads effect on a foundation for a 100-meter-high wind turbine with meteorological data measured at Kvitneset, Norway, in an open coastal landscape, for every 10-minute interval during one year at three different heights. Then, the author applied the requirements of three different standards: DNV-OS-C502, Model Code 2010 and NS-EN 1992-1-1 [14,37,42]. It was found that deviations exist in the results for compression and shear, indicating that concrete fatigue needs further development and better standardization.

Grouted connections, as well as concrete, are also subjected to dynamic loads in wind turbine structures. These connections are represented in a scheme in Fig. 6a. The materials used to link the wind turbine foundation to the transition piece, which is directly bolted to the tower (Fig. 6a), may also degrade due to fatigue. It has been stated that the capacity of these connections to support the repetitive loads (wind or waves) decreases with time [43].

Fatigue can be understood as a physical phenomenon characterized by progressive and irreversible wear or deterioration, which occurs in the material, characterized by the slow growth of one or more cracks under the action of cyclic loading, eventually leading to fracture [4,7,44]. Whether concrete or grout, the fatigue of these materials follows the same process and occurs in two stages before failure Fig. 6b. The first step is the nucleation of cracks (1), which corresponds to the formation of small cracks that could be seen on the surface. The second step is the crack growth (2), where the cracks grow slowly inside the materials affecting negatively the strength. This phase is followed by the fracture (3) which marks the failure of the structure by fatigue. A classification of structures according

to the typical number of cycles to failure that can be observed was given by [45] and illustrated in Table 1. It gives three fields of fatigue depending on the structure.

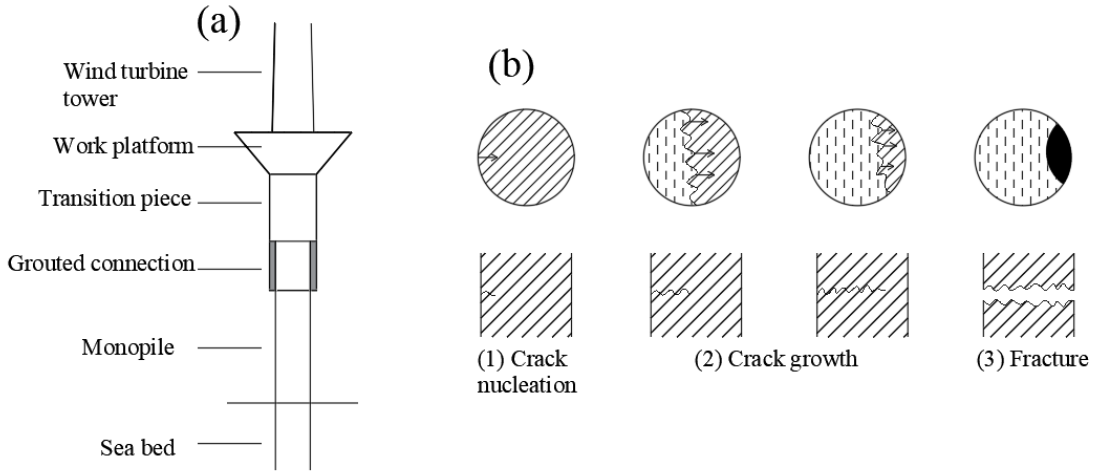

Fig. 6: Scheme of (a) the connections between the foundation and the tower, (b) phases of fatigue process.

Table 1: Classification of structures according to fatigue loads given by [45]

Low-cycle fatigue			High-cycle fatigue		Super-high-cycle fatigue				
1	10^1	10^2	10^3	10^4	10^5	10^6	10^7	10^8	10^9
Structures subjected to earthquakes			Airport pavement and bridges		Highway; railway bridges and highway pavements		Mass rapid transit structures		Sea structures

Under dynamic loads, the fatigue strength of materials is evaluated from the number of cycles to failure (N*f*), obtained by the construction of semi-logarithmic curves representing the maximum applied stress level (S_{max}) as a function of N*f*, called Wöhler (or S-N) curves. These curves represent the relationship between the magnitude of applied stresses and the number of loading cycles required to produce failure N*f* at that specific stress magnitude. According to Lee and Barr [4], these curves were developed by Wöhler between 1852 and 1870 [25] when studying the fatigue behavior of railroad steel structures. Fatigue failures are obtained by applying repeated loads at different stress levels with amplitudes below the required stress to failure in one cycle (static strength). For each test, a number of cycles to failure is reached and the S-N diagram receives another data point. To avoid a possible excessive effect of dispersion on the results, Paskova and Meyer [46] based on statistical data, showed that at least 5 specimens per tested loading magnitude should be tested to establish a S-N curve. At least three different stress ranges should be selected in the S-N region of interest so that a representative slope of the S-N curve can be determined [9]. In the case of non-availability of a sufficient number of specimens, Sainz-Aja et al. [47] have proposed a comparison and a correlation

between two methods : (1) Locati's method [48], which is based on Miner's hypothesis, and allowing to estimate the fatigue limit by using a single piece, subjected to load steps of the same duration, and (2) the Staircase's method. The purpose of their study [47] was to estimate the fatigue limit of three types of concrete made from recycled aggregates. The two methods show almost the same results. However, Locati's method is more advantageous with a fatigue limit of 2.10^5 cycles per step, proposing a reduced number of tests, which makes the studies more economical in terms of time and cost. In order to achieve this latter objective, [49] proposed a method which consists of applying loads at a frequency up to the resonance frequency of the system (specimen + testing machine). The tests were performed on concrete with recycled aggregates. This method proved to be more conservative. In addition, the resonance frequency was found to be a relevant parameter to identify the variations of stiffness of the system, and also to indicate the failure of the specimen.

Some equations have been developed to estimate fatigue life from the number of cycles to fatigue for ordinary concretes of strength classes lower than C80 [37]. As shown in Fig. 7, these equations describe the fatigue behavior by a relationship between the applied stress and the number of cycles to failure. To consider the difference between the most common standards: CEB-FIP Model, DNV-OS-H101 and Eurocode 2 [9,35,36], we plot the S-N curves from three standards for S_{max} = 1 and S_{min} = 0.2. It is observed that the standard DNV-OS-H101 [36] underestimates fatigue life compared to the other calculation procedures.

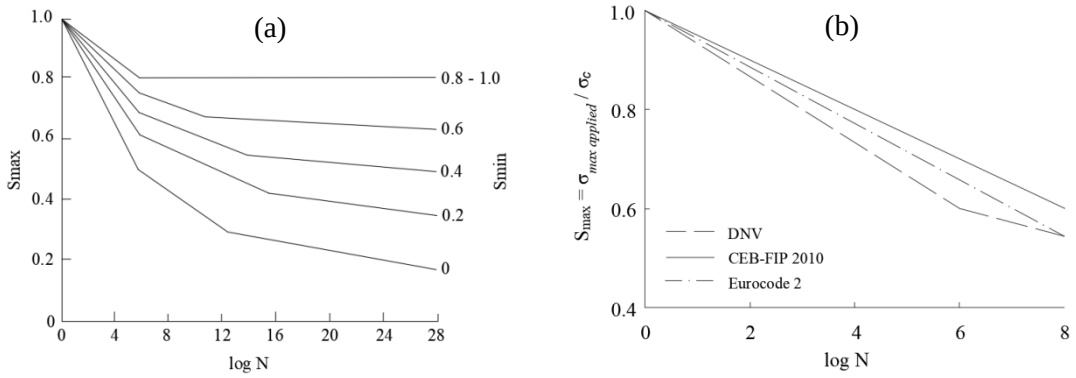

Fig. 7: (a) S-N curves from CEB-FIP, 2010 [9], (b) Comparison of S-N curves from 3 standards.

Fatigue progression is accompanied by strain development in the material during fatigue tests, as illustrated in Fig. 8a. Failure occurs when the stress-strain curve reaches the point in the descending branch of a stress-strain diagram containing the fatigue failure envelope. Fig. 8a also represents stress-strain cycles (with predominantly compression loadings), with degrading modulus (decreasing slope on stress-strain diagram). It represents possible static stress-strain paths, with similar slopes as after cyclic loading, and that leads to failure at decreased maximum nominal stresses (descending branch of the failure envelope). In addition, Fig. 8c represents an experimental cyclic stress-strain curve for compression tests performed in our project described previously. Meanwhile, Fig. 8b represents the

evolution of the maximum axial strain with the number of cycles N. This occurs in three phases (Fig. 8b). Phase I corresponds to an accelerated increase of the strain level, obtained for fixed stress level during the cycles, associated with the nucleation of cracks. Microcracks form at the aggregate-paste interface, leading to substantial damage to the concrete properties. It corresponds to about 10-20% of fatigue life. It is accompanied by the degradation of the fatigue secant modulus [50]. The authors show a great drop in the secant modulus with the degradation of material by fatigue loads (Fig. 8d). Then, Phase II may show a change in strains, depending on the average stress (if there is compression, for example). It ends at about 80-90% of fatigue life. During the second stage, microcracks develop regularly, while the strain increases at a constant rate and the modulus of deformation decreases, also at a constant rate. Phase III is characterized by a very rapid increase of the strain (if there is compression, for example), causing the sample failure at the number of cycles N*f*. During the final stage, the microcracks converge to form a macrocrack that leads to the failure of the specimen. It is crucial to note that some authors consider N*f* as the actual beginning of this last phase and associate that with the coalescence of microcrack into a macrocrack. This is done because rigorously it places the study out of the Mechanics of Continuous Media field (because there is already a macrocrack in the material), where bulk parameters (such as stress and strain fields and material properties such as the modulus) cannot be rigorously obtained from the measured loads and displacements during the tests [7,51]. Substantial material deterioration also occurs during this third stage.

During fatigue tests, material heating is observed [5,52,53] and this may be associated with micromechanical friction. For viscoelastic materials, this is classically associated with the viscous part of the material behavior and can be calculated after modeling of viscoelastic properties [51,54]. Holmen [55] observed that, at each cycle of reloading, the elastic deformation increases through the reduction of the secant modulus of elasticity. The transversal deformability was also affected since the Poisson coefficient increased during the fatigue test. After providing a theoretical description of the stress and strain evolutions, and in order to better understand, experimentally, the fatigue behavior in terms of stress and strain, compressive fatigue tests have been applied by Viswanath et al. [56] on Normal Strength Concrete (NSC). They observed a non-linearity in the second phase of the strain evolution. A high magnitudes of strain gradient were noted at the initial and the third phases, which decreased toward the second phase. Viswanath et al. [56] also presented the evolution of the peak strain and showed that it is affected by the number of cycles to failure N*f*, showing that a large N*f* exhibits large strain magnitudes. This latter is also affected by the maximum stress level S_{max}. Thus, an increase in this latter leads to an increase in the peak strain evolution ε^{max}.

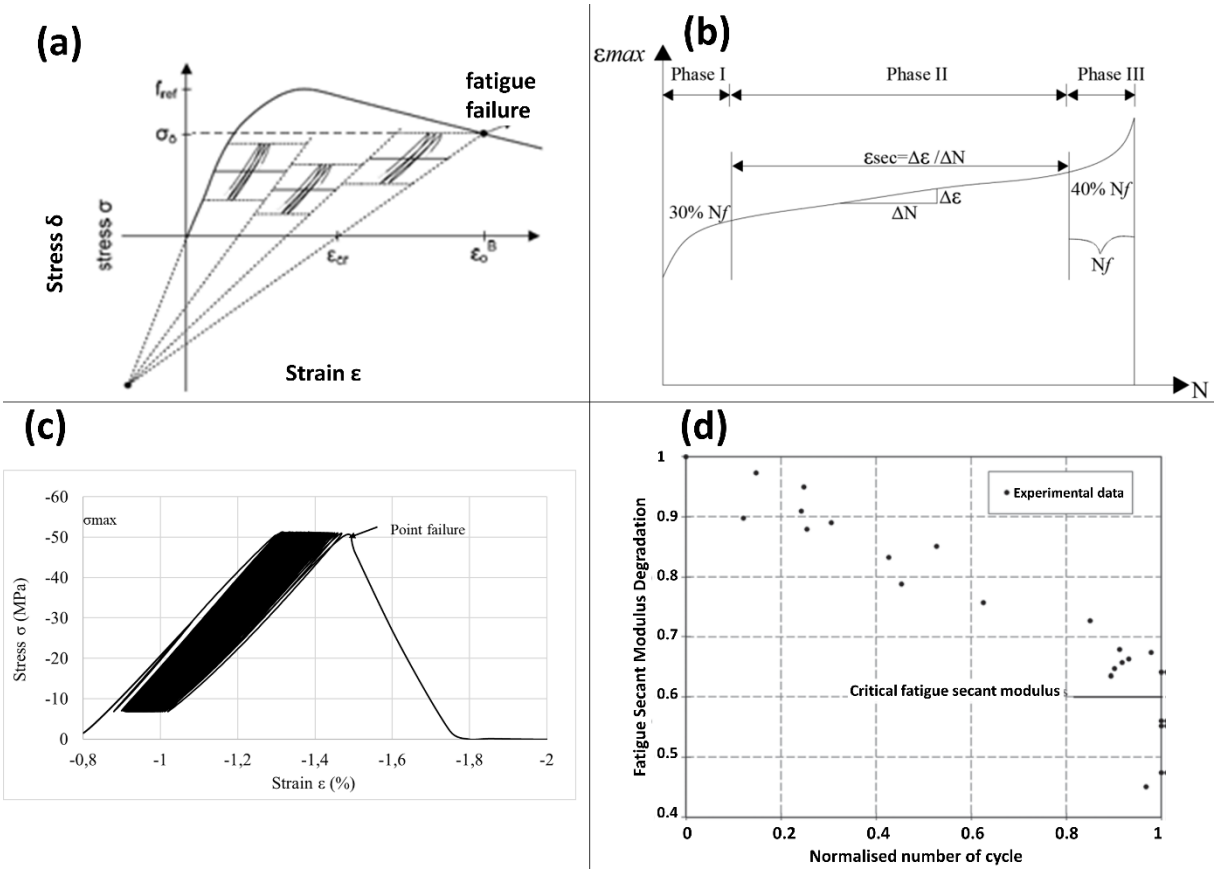

Fig. 8: (a) Idealized fatigue stress-strain curve (Park, [57]), (b) Evolution of strain as a function of the number of cycles, (c) Experimental stress-strain obtained from fatigue tests on a sample of foundation wind turbine analysis, (d) Degradation of secant modulus by fatigue loading (Isojeh et al., [58]).

III.3. Fatigue models

Several phenomenological and mathematical models of concrete fatigue behavior were reported in the literature. Among others, it includes the work of Baktheer and Chudoba [59] in which works related to numerical modelling are grouped. Reviewing the literature on numerical investigations for concrete fatigue behavior, three widely used models are identified as part of two approaches. The first one named "Lifetime based approaches" focuses on the fatigue behavior of concrete and is described in terms of the loading cycles performed. Meanwhile, the second one is based on the theory of fatigue damage mechanics coupled with strain measurement named "Strain based approach".

III.3.1. Fatigue behavior modelling by lifetime-based approach

III.3.1.1. Strain approximations

Analytical and empirical models have been developed by [50,58,60–67]. The fatigue behavior has been described in this class of models in term of fatigue lifetime scale. Indeed, the strain evolution during fatigue life is defined as a function of the number of cycles as follows in Eq. (5):

$$\varepsilon^{max}(N)=\varepsilon^{0}+\lambda\left(-ln\left(1-\frac{(N-1)}{N_f}\right)\right)^{1/k} \quad (5)$$

where, ε^{max}, N, N_f and ε^{0} are the strain evolution, cycle's number, number of cycles at failure and maximum strain, respectively. λ and k are the coefficients to be calibrated based on experimental observations to obtain the fatigue creep curves.

Then, the fatigue strain rate can be obtained as follows in Eq. (6):

$$\frac{\partial\varepsilon^{max}}{\partial\left(\frac{N-1}{N_f}\right)}=\frac{\lambda}{k}\frac{1}{1-\left(\frac{N-1}{N_f}\right)}\left(-ln\left(\frac{1}{1-\left(\frac{N-1}{N_f}\right)}\right)\right)^{1/k-1} \quad (6)$$

The strain evolution and the fatigue strain rate are illustrated in Fig. 9 (Huang et al. [62]). As noted previously, ε_0 is the fatigue deformation of the first cycle [see Point A in Fig. 9a]. It can be found that if the value of the load cycles ratio $\left(\frac{N-1}{N_f}\right)$ is set to *1-1/e*, the fatigue deformation is equal to $\varepsilon^{0}+\lambda$ [see Point B in Fig. 9a]. Indeed, λ may reflect the degree of fatigue creep deformation, and it can be termed the fatigue creep parameter. As seen in Fig. 9, the models represent rather adequately the phenomenological observations on the fatigue behavior of concrete materials, as previously described in Section II.2. It is also noted that the strain rate, known as the secondary strain rate, can be considered as a constant in this stage, given the fact that the deformation increases almost linearly. Such parameter is defined as the slope of the fatigue deformation curve along Stage (II) as shown in Fig. 9 b and given by Eq. (6). Therefore, for the strain versus ratio of load cycles curve, the strain rate at point B is considered as the secondary strain rate. Considering Eq. (6), the fatigue strain rate at Point B can be derived as follows in Eq. (7):

$$\left.\frac{\partial\varepsilon^{max}}{\partial\left(\frac{N-1}{N_f}\right)}\right|_{1-1/e}=\frac{\lambda}{k}e \quad (7)$$

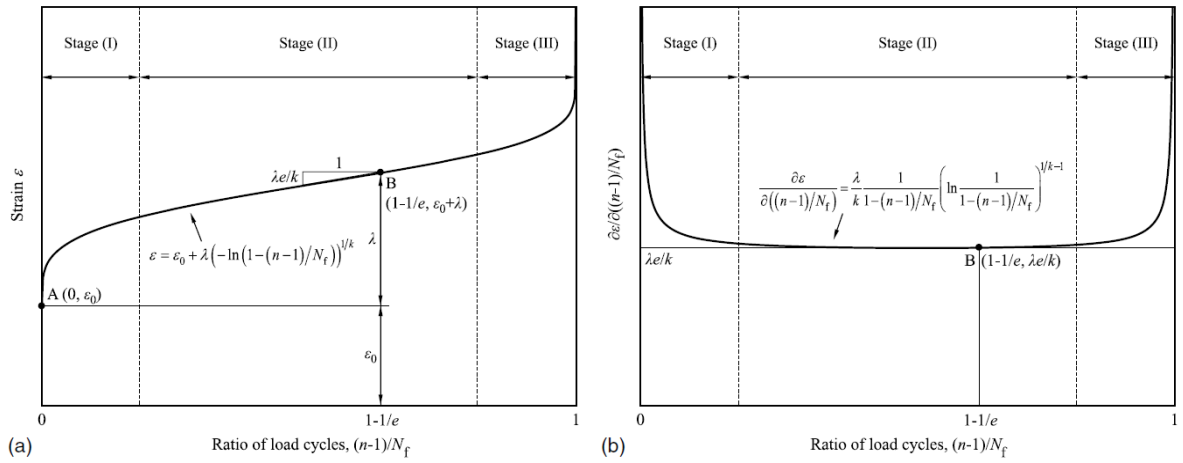

Fig. 9: Physical meaning of model parameters based on (a) ε^{max} *vs.* $\frac{N-1}{N_f}$ *;(b)* $\frac{\partial \varepsilon^{max}}{\partial\left(\frac{N-1}{N_f}\right)}$ *vs.* $\frac{N-1}{N_f}$ *(Huang et al.*[62]*)).*

It can be noted that the secondary strain rate is determined by the value of λ/k. A concrete having a high value of λ/k corresponds to a faster fatigue-induced microcracks propagation under microscope. In this model, the rate of change of the strain rate might be used to define the changes of fatigue stages because the variation rates at the first and third stages are much higher than that of the second stage [Fig. 9b].

Due to the simplicity of this model class, the lifetime stress prediction of concrete fatigue remains unreliable under other types of loading, i.e., the material coefficients need to be calibrated again for each type of loading. This limitation presented by these approaches is due to the fact that it neither faithfully describes the macroscopic behavior nor reflects the dissipative mechanisms governing the propagation of fatigue damage in concrete, which limits their use.

III.3.1.2. Damage approximations

Phenomenological models were proposed by [68–71]. In this class of models, the fatigue damage is modeled by a function and using the number of performed loading cycles as follows:

$$\omega = f(N, S_{max}, S_{min}) \tag{8}$$

where $\omega, S_{max}\ and\ , S_{min}$ are the fatigue damage function, the upper and the lower fatigue loading levels, respectively. The damage plasticity framework was employed with explicitly specified relation between fatigue damage and number of uniform loading cycles was introduced. However, this damage hypothesis has been criticized due to conflicting experimental observations [72,73].

However, the model can reproduce the macroscopic variations in concrete as the number of cycles rises in simplified form as shown in Fig. 10 (Zanuy et al. [73]). The equations proposed to relate maximum strain (ε_{max}) and the modulus of deformation (E) to the number of cycles can be expressed by Eqs. (9 – 12), as follows:

$$\varepsilon_{max}\left(N = 0.1N_f\right) = \frac{1.18\ \varepsilon_0}{S_{max}} \tag{9}$$

$$\frac{\partial \varepsilon^{max}}{\partial\left(\frac{N}{N_f}\right)}\left(0.1N_f < N < 0.8N_f\right) = \frac{0.74\ \varepsilon_0}{S_{max}} \tag{10}$$

$$E\left(N = 0.1N_f\right) = [(0.09 + 8.19S_{min}) + (0.84\ -\ 8.19S_{min})S_{max}]E_c \leq 0.93E_c \tag{11}$$

$$\frac{\partial E}{\partial\left(\frac{N}{N_f}\right)}\left(0.1N_f < N < 0.8N_f\right) = \frac{0.25}{0.61 - S^{min}}\left(0.39 + S^{min} - S^{max}\right)E_c \leq 0 \tag{12}$$

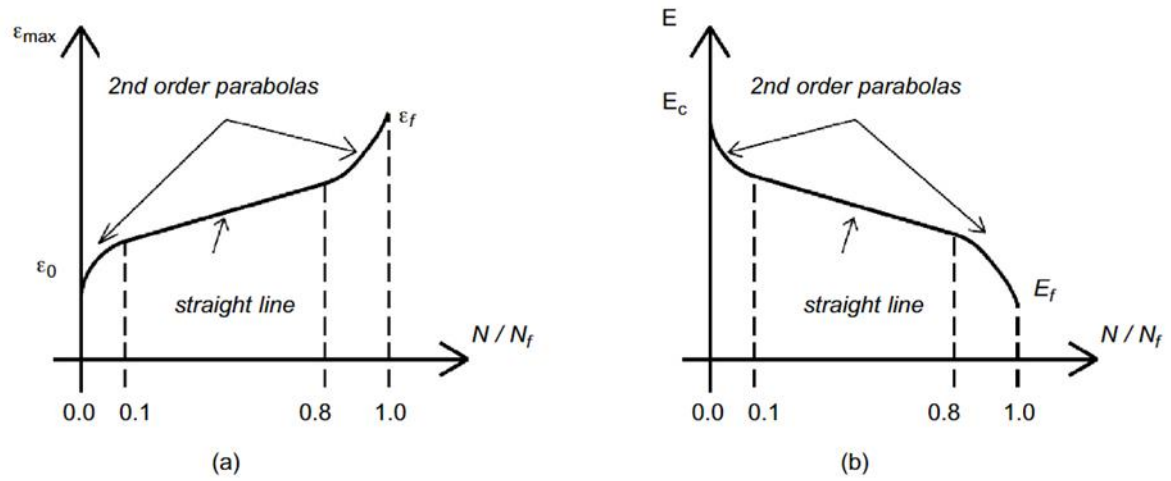

Fig. 10: Fatigue evolution laws for: (a) total strain; (b) modulus of deformation (Zanuy et al. [73]*).*

The damage degree indicated by the model parameters is related to the maximum and the minimum stress values (S_{max}, S_{min}). Again, it is seen in Figs. 10a and b that the models represent adequately the phenomenological observations on the fatigue behavior of concrete materials, as previously described in Section II.2.

III.3.2. Fatigue behavior modelling by strain-based approach

III.3.2.1. Macro-scale tensorial models

In this model class, the damage-plasticity framework is used to establish tensor relations between strains and stresses using the constitutive equations representing the behavior laws [74–76]. Due to the development of powerful computing resources in the last decades, the simulation of the fatigue damage process has become possible. Moreover, the standard framework of viscoplasticity modeling has been mentioned by Marigo [76], who proposed the replacement of the traditional yield strength with an irreversibility condition to reflect the loading/unloading behavior. In this case, the fatigue damage is governed by an equivalent strain measure such as

$$\omega = f(\dot{\varepsilon}^{+}) \qquad (13)$$

where $\dot{\varepsilon}^{+}$is the positive rate of the equivalent strain.

A related method was also carried on by Mai et al. [77], who introduced the evolution of the damage in the form of a power law of an equivalent strain rate. Also, the fatigue damage is related to inelastic strain [78]. Indeed, a three-dimensional phenomenological model is developed to describe the fatigue behavior of concrete. The approach is based on the framework of continuum damage mechanics, where the fatigue model is derived by means of Marigo's formulation [76], where the yield concept is replaced by a loading–unloading irreversibility concept allowing to account for damage accumulation even for loading levels below the yield surface. Following the concept of effective stresses and the principle of strain equivalence, the stress in the damaged material induces the same deformation as the

effective stress in the undamaged material. They are related through the damage variable ω, as in Eq. (14). Moreover, the total strain is given by Eq. (15) regrouped the elastic and inelastic strain and are related to the stress via the constitutive equations as given by Eq. (16).

$$\sigma=(1-\omega)\bar{\sigma} \tag{14}$$

where σ, ω and $\bar{\sigma}$ are stress tensor, damage variable and effective stress tensor, respectively.

$$\varepsilon=\varepsilon^{e}+\varepsilon^{in} \tag{15}$$

$$\bar{\sigma}=C:\left(\varepsilon-\varepsilon^{in}\right) \tag{16}$$

In the work of Kindrachuk et al. [78], the simulations of a strain-controlled test is rather straightforward because the derived implicit integration scheme presumes a known strain increment. Furthermore, the strain increment is a priori unknown for a stress-controlled simulation, and they have been found via the inverse method. The stress equilibrium and the strain increment were found iteratively by applying the algorithmic tangent as the Jacobian matrix. In each time step the strain increment $\Delta\varepsilon^{[k]}$ (in the [k]-th iteration) is related to the applied stress increment $\Delta\sigma$ as given in Eq. (17). and the updated strain increment is calculated by the gradient descent method given by Eq. (18).

$$\Delta\sigma\left(\Delta\varepsilon^{[k]}\right)-\Delta\sigma+\frac{\partial\Delta\sigma\left(\Delta\varepsilon^{[k]}\right)}{\partial\Delta\varepsilon^{[k]}}:\delta\varepsilon^{[k]}=0 \tag{17}$$

$$\Delta\varepsilon^{[k+1]}=\Delta\varepsilon^{[k]}+\delta\varepsilon^{[k]} \tag{18}$$

where $\delta\varepsilon^{[k]}$ is the variation step of strain.

III.3.2.2. Meso-scale microplane models

Microplane model formulation can be considered as a coupled multiscale model with introducing an additional level of state representation below the level of material point [79]. This can reflect the damage and its anisotropic evolution as the loading progresses. Furthermore, it applies the concept of kinematic stress and stress homogenization to relate the macroscopic and microplane level of discretization with tensor and vector representation of the material state, respectively [79–82]. The main idea of this model is to relate the damage evolution to the cumulative strain measurement. As the state variable determining the damage evolution, the researchers chose the path length of the total volumetric strain over the loading history. This model was validated and compared with a series of three-point bending tests of different sizes.

$$\omega=f(\varepsilon^{v,cum}) \tag{19}$$

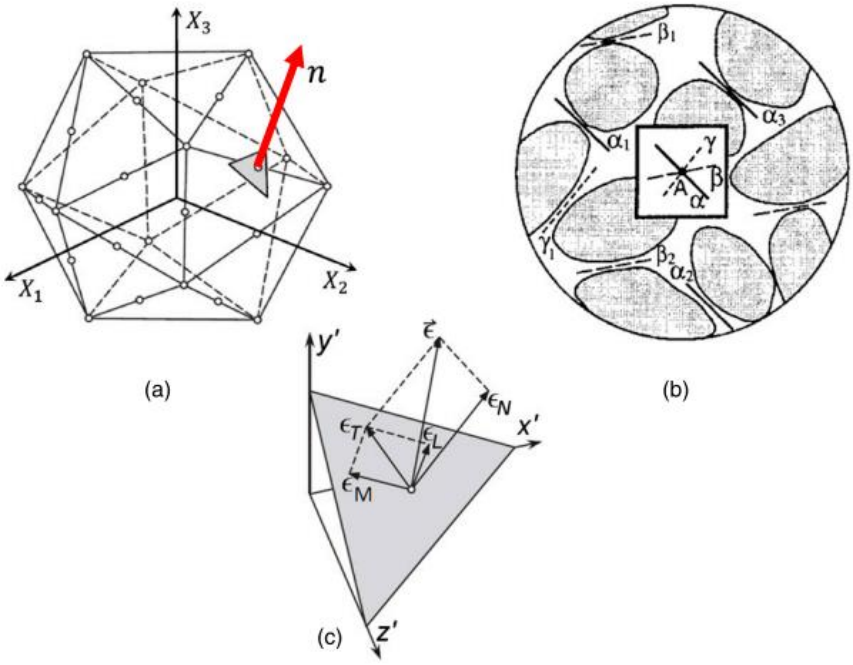

Fig. 11: (a) Microplane strain vector and its components; (b) system of discrete microplane; (c) microplane strain components [81].

The hypothesis established by Bazant and Gambarova [83] shows the need to ensure the post-peak strain softening stability and thus the use of a robust explicit algorithm. The strain vector ε_N on the microplane (Fig. 11a) will be the projection of ε, i.e., $\varepsilon_{Ni} = \varepsilon_{ij}\, n_j$, where n_i are the components of the unit normal vector n of the microplane, with the subscript i refers the global Cartesian coordinates x_i *(i= 1, 2, and 3)*. The orthogonal unit coordinate vectors m and l, of components l_i and m_i, that lie the microplane is introduced [Fig. 11c]. Taking the projections of vector ε_N onto n_i, l_i, and m_i, the normal and shear strain components and the resultant of the shear strain are defined as in Eqs. (20,21):

$$\varepsilon_N = N_{ij}\varepsilon_{ij},\ \varepsilon_L = L_{ij}\varepsilon_{ij},\ \varepsilon_M = M_{ij}\varepsilon_{ij} \qquad (20)$$

$$\varepsilon_T = \sqrt{\varepsilon_L{}^2 + \varepsilon_M{}^2} \qquad (21)$$

where $N_{ij}=n_in_j$, $L_{ij}=(l_in_j+ l_jn_i)/2$, $M_{ij}=(m_in_j+ l_jn_i)/2$.

The index *N, L and M* denote the normal direction n_i; and the shear directions l_i and m_i respectively. The index t denotes the shear resultant. Summation repetition over i= 1, 2, and 3 is implied by the repetition of the indexes. A vector m_i is chosen to be normal to the x_3-axis, in which case $m_1 = n_2 / (n_1^2+ n_2^2)^{1/2}$, $m_2= -n_1 / (n_1^2+ n_2^2)^{1/2}$, $m_3=0$, but $m_1=1$ and $m_2= m_3=0$ if $n_1= m_2=0$. A vector m_1 normal to x_1 or x_2 is obtained by permuting the indexes 1, 2, and 3. The orthogonal unit vector is generated as $l = m \times n$. However, to minimize directional bias, vectors m are alternatively chosen to be normal to the x_1-, x_2-, or x_3-axes. To model the damage in compression, it is useful to define the deviatoric normal strains ε_D on the microplanes, as in Eq.(22).

$$\varepsilon_D = \varepsilon_N - \varepsilon_V,\ \varepsilon_V = \varepsilon_{kk}/3 \qquad (22)$$

where ε_V is the volumetric strain (or mean strain), which is the same for all the microplanes. In general, the static equivalence, or equilibrium, between the stress vectors on all the microplanes and the stress tensor must be applied in variable way, according to the principle of virtual work the strain energy is written as in Eq. (23) [83].

$$\frac{2\pi}{3}\sigma_{ij}\delta\varepsilon_D = \int_\Omega (\sigma_N \delta\varepsilon_N + \sigma_L \delta\varepsilon_L + \sigma_M \delta\varepsilon_M)\, d\Omega \quad (23)$$

where Ω is the surface of a unit hemisphere centered at the material point; and 2π/3 its volume. This equation means that the virtual work of stresses (or macrostresses) of the continuous medium within a unit sphere must equal the virtual work of the microplane stress components (or microstresses) considered as the tractions on the surface of the unit sphere. The integral can be displayed as directed homogenization of the contributions from planes of different orientations within the material, as shown in Fig. 11b. Following a formal development, it is possible to obtain Eqs. (24,25).

$$\sigma_{ij} = \frac{3}{2\pi}\int_\Omega s_{ij} d\Omega \approx 6\sum_{\mu=1}^{N_m} w_\mu {s_{ij}}^{(\mu)} \quad (24)$$

$$s_{ij} = \sigma_N N_{ij} + \sigma_L L_{ij} + \sigma_M M_{ij} \quad (25)$$

From the point of view of numerical calculations, the above integral is approximated by an optimal Gaussian integration formula for a spherical surface (Bazant and Oh [84]) representing a weighted sum over the P microplanes of orientations n_μ, with weights w_μ normalized such that $\sum_\mu w_\mu = 1/2$ [84,85]. However, the most efficient formula that still yields acceptable accuracy involves 21 microplanes (Fig. 11b) ([84], although to obtain better accuracy in the far postpeak softening, selecting 37 microplanes is preferred based on the work of Bazant et al. [81]. Then, the model's parameters are given in Eq. (26).

$$E_N = \frac{E}{1-2\nu}, \quad E_T = E_N \frac{1-4\nu}{1+\nu} \quad (26)$$

where ν, E_N and E_T are Poisson's ratio and Young's modulus, longitudinal and transverse at the macro scale respectively.

III.3.2.3. Meso-scale discrete models

During the last two decades, simplified models have been proposed with a single rigid body associated with each grain. Discrete schematization of the material structure leads to fine modeling of elementary dissipative effects. Indeed, in terms of displacement discontinuities (fractures and cracks) or development of transverse tensile stress under compressive loading (separation cracks), this models provides valuable insight into the phenomenology of elementary decay mechanisms in the material structure and can help formulate appropriate damage assumptions at higher modeling scales [86–88]. The main advantage of such an approach is the significantly lower computational complexity [89,90]. However, the direct application of this type of model to cyclic loading is not usually done. Grassl and Rempling [91] studies the fundamental mechanisms of damage evolution for cyclic compressive loading. Moreover, Guo et al. [86] focuses on compressive fatigue.

A stochastic physical model for concrete damage under fatigue loading has been proposed by [92,93] . Based on the stochastic mesoscopic fracture model (MSFM), a failure criterion for meso-elements under fatigue loading is established, which assumes that the energy dissipation of a meso-element from its initial state to its failure state is certain for the monotonic or fatigue loading process. A representative volume element (RVE) of concrete can be modeled as a series of springs, or meso-elements, joined in parallel (Fig. 11). The springs are supported at either end by rigid bars so that they can extend equally under axial loading. Each of them is considered to be perfectly elasto-brittle with equal elastic stiffness E_0 and the fracture strain of the springs Δ is considered to be a random field (Fig. 12). Therefore, if the total number of the springs is denoted as X and the spatial coordinate x of the i^{th} spring is expressed as $(i-1)/X$ $(i=1,2, \ldots, X)$, then the damage of the above RVE can be defined as the ratio of number of failed springs, n, to the total number of springs, as presented in Eq. (27):

$$d = \frac{n}{X} = \frac{1}{X}\sum_{i=1}^{X} H(\varepsilon - \Delta_i) \tag{27}$$

where H is the Heaviside function. When number of springs X approaches to infinite, it can be written as in Eq. (28). Then, the one-dimensional constitutive relationship of the RVE is obtained as in Eq. (29).

$$d = \int_0^1 H(\varepsilon - \Delta)\, dx \tag{28}$$

$$\sigma = (1-d)E_0\varepsilon \tag{29}$$

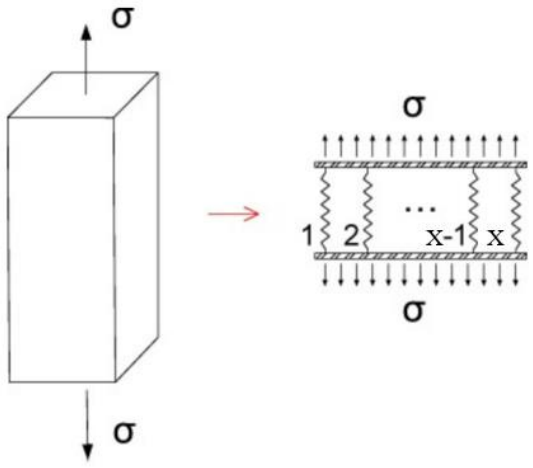

Fig. 12: Modelled element.

After that, to obtain the energy dissipation rate of meso-elements, an energy analysis of one growing nano-crack is conducted by employing the classical rate process theory, and the number of nano-cracks distributed in a meso-element is hypothesized to follow a power law of the nanoscale's stress state. Finally, the stress applied on nano-elements is discovered to be coupled with the fracture strain of meso-elements. The MSFM can be established as in Eq. (30).

$$W_i = \Omega_i = \frac{1}{2}E_0{\Delta_i}^2 \tag{30}$$

where W_i is the cumulative energy dissipation of the i_{th} meso-element under fatigue loading and Ω_i the fracture energy release of the i_{th} meso-element when it fails under monotonic loading E_0.

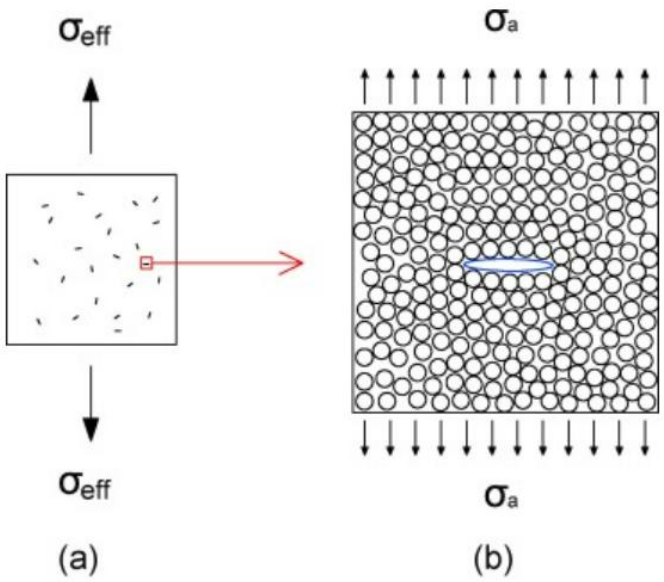

Fig. 13: (a)Meso-element; (b) Nano-crack element.

The original and still most recognized models (often called lattice models) distinguish the entirety of concrete phases (grain, void, cement paste, and interface transition zone (ITZ) between grain and cement paste). These latter require robust resolution of the underlying discretization and thus require significant computational resources. They have been applied to a wide variety of problems, including fracture, elasticity, high and low temperature, dynamics, or transport phenomena [91,94,95].

IV. Effect of fatigue parameters on the dynamic behavior of materials

Concrete fatigue is affected by several parameters, namely the loading frequency; the environment in which the concrete will be manufactured and then loaded (dry environment for onshore wind turbines, or wet environment for offshore wind turbines); and the size of the samples. Several studies have taken these factors into account and obtained results that are sometimes contradictory and/or complex to interpret due to the interference of different parameters simultaneously on the behavior. Some works have studied several parameters simultaneously on the same samples to evaluate the effect of each of them on material fatigue [5,26]. Many other studies are also discussed in the following sub-sections. This section is organized using parameters mainly taken from the two aforementioned studies, but with a discussion concerning the results from many other research papers. Only the significant studies are detailed in this section, for the rest, a brief description of the significant results is given.

Oneschkow et al. [26] studied the behavior of a high strength concrete (HSC), with 8 mm maximum grain size of the aggregate, under dynamic loads. The class of compressive strength of C80/95 has been obtained from compressive tests on cubic specimens of 150x150x150 mm^3. Fatigue tests were conducted considering the compressive load as being uniaxial sinusoidal (Fig. 5a). These tests were

carried out on cylindrical specimens of 60-mm diameter by 180-mm height, and 100-mm diameter by 300-mm height, by two servo hydraulic testing machines of 1 and 2.5 MN capacity. The authors studied the effects on the fatigue resistance of the material of (i) five stress levels (S_{max}), which were kept constant for the whole test; (ii) three loading frequencies; (iii) two environmental conditions; and (iv) two specimen sizes. Only the maximum stress level varies, while the minimum stress level S_{min} = 0.05 was kept constants for all the tests.

Myrtja et al. [5] have also studied the behavior of a grout under dynamic loading in compression. 50 samples of dimensions 60-mm diameter by 120-mm height were tested after 8 weeks of their confection with compressive strength of 168 MPa, at different stress levels Smax (0.70, 0.75, 0.80, 0.85, and 0.90) and at two testing frequencies (1 and 10 Hz). The minimum stress level was kept constant at 0.10.

The results of each parameter are given in paragraph III.1 for the loading frequency, III.2 for the environmental conditions, and III.3 for the specimen sizes, for different maximum stress levels. Then, in paragraph III.4, the effects of other parameters are discussed. Finally, in paragraph III.5, the heating phenomenon during tests is presented. Other authors, focused on each of the commented aspects, will be also cited and their results commented.

To characterize crack formation due to fatigue loading, Golewski [96] has identified the main material parameters affecting the behavior of reinforced concrete under fatigue loading, which can mainly be summarized as follows: the energy of vibration absorption, the damping coefficient, other mechanical properties, and particularly fatigue strength. They have shown that the propagation of cracks is significantly important through aggregate grains than in the ITZ area.

IV.1. Loading frequency

Murdock [97], in his critical review, affirms that studies conducted before 1965 showed no or a little effect of frequency on concrete fatigue. A recent study by Soerensen et al. [98] also pointed in the same way. Nevertheless, loading frequency is one of the most important parameters to consider when dealing with cyclic loads. It has been suggested as an important parameter on the dynamic behavior of concrete since the 1960s [99], which has then been confirmed in the 1970s [100,101] to be later considered analytically in the calculations.

Several authors have studied the effect of loading frequency on the dynamic behavior of materials [5,6,26,52,72,97,101–112]. Some contradictions in the conclusions are noted. Graf and Brenner [21] were the first to evaluate the effect of frequency on the fatigue behavior of concrete, according to Zhang et al. [112]. As described previously, they found that the effect of loading frequency on the fatigue life is not very significant, especially at higher frequencies. Fig. 14 describes a temporal evolution for loading frequency effect on materials.

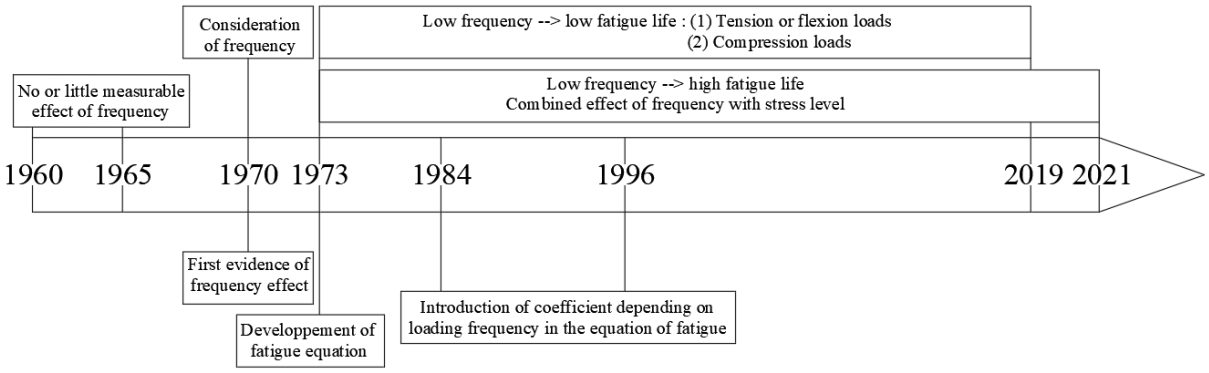

Fig. 14: Timeline of consideration of loading frequency as an influencing parameter on fatigue life.

Some authors [103,112] showed that low loading frequency induces low fatigue of concretes subjected mainly to tension or to bending. Zhang et al. [112] applied flexural cyclic loads on concrete beams for six different loading frequencies 0.5, 1, 5, 10, 20, and 30 Hz. Two series of tests were conducted with constant stress ratios of 0.20 and 0.80. A new fatigue equation was developed from Eq. (1), to consider the effect of frequency. A coefficient has been introduced to this equation in order to consider the effect of frequency (cf. Eq. (3)) on the fatigue equation developed previously. They showed that this coefficient increases with increasing frequency allowing high fatigue life. This could be explained by the effect of a high loading frequency on increasing stress and strain rates, which generates strength growth, showing that there is a viscous effect on the damage behavior [113].

For pure compression tests, the authors [6,52,101,105,109,111,114,115] have reached similar conclusions. According to Hümme et al. [52] and Holmen [55] also acknowledged the influence of loading frequency of plain concrete. This was not the case for Klausen [116] who could not observe this effect for $S_{max} < 0.80$.

Some parameters, such as frequencies, stress levels, and temperature increase, could have a combined effect which is even more significant considering the results. In this sense, many authors [101,106,108] showed a short fatigue life of concretes subjected to low-stress levels and high loading frequency. This effect is reversed as the maximum stress level increases, as expected. This was confirmed in recent studies on high-strength concrete [52,72,110], and on grout by [107] and was explained by the increase in sample temperature caused by high frequencies. Some authors find no effect of frequency for low stress levels; [97,104] have shown that when S_{max} is less than 0.75, frequencies between 1 and 15 Hz do not have much influence. Meanwhile, Sparks and Menzies [101] state that for a value of S_{max} between 0.75 and 1, the frequency greatly affects the number of cycles to failure. However, when S_{max} is low, frequencies have no effect. Therefore, all these authors state that for low stress levels S_{max}, the effect of frequency is negligible, and effect arise when stress levels increase. Oneschkow et al. [26] studied three different loading frequencies (0.1, 1, and 10 Hz) for dry

environment, and two loading frequencies (1 and 10 Hz) for wet environment on the specimens of 60 mm diameter by 180 mm height. They found that for a stress level $S_{max} \geq 0.8$, the number of cycles increases with frequency and that this effect is more pronounced in wet environment for all stress levels. However, for $S_{max} < 0.8$, the effect is reversed showing that the number of cycles is larger for low frequency. For this case, this was explained by the authors by a higher concrete age of the specimens tested at the low frequency of 1 Hz. However, Myrtja et al. [5] have also found results in this sense, showing a slight increase in the number of cycles at low frequency (1 Hz), for $S_{max} = 0.75$. The latter authors explained the phenomenon by a temperature rise, which was more important for the tests with lower stress levels, at $f = 10$ Hz. They followed the temperature evolution induced by fatigue loading, which indicated a more pronounced rise of temperature at low stress levels ($S_{max} = 0.75$). This increase was probably the cause of this slight reduction on the fatigue strength. Consequently, this explains the decrease in the number of cycles at high frequency (10 Hz) for low stress levels.

Medeiros et al. [105] presented an experimental study of fatigue behavior of concrete with gravel aggregate of 12 mm as maximum size, using 123 cubic specimens under four loading frequencies (4 Hz, 1 Hz, 1/4 Hz, 1/16 Hz) for $S_{max} = 0.85$. The stress ratio of 0.3 was kept constant. They tested three types of concrete: plain concrete, polypropylene fiber reinforced concrete, and steel fiber reinforced concrete having a strength of 79 ± 4 MPa, 74 ± 6 MPa and 89 ± 3 MPa, respectively. The tests were conducted using a servo-hydraulic testing machine equipped with two LVDT (Linear Variable Differential Transducer) to measure displacements. A large scattering of results (Fig. 8a) was observed on several samples with the same properties and under the same conditions [105]. However, the majority of results indicate that the number of cycles to failure increases with the frequency, which is less important for plain concrete. This increase of Nf was confirmed by three models and represented by Medeiros et al. [105] in his paper (Fig. 15b), which led the authors to represent the probability density function corresponding to each loading frequency. Additionally, their results highlight the positive effect of fibers addition on increasing the fatigue strength of concrete, except for the 4 Hz frequency. About deformations, they showed that for high strain rates, the fatigue life is low. The probability density function is used to consider the dispersion of the results. By comparing their results with numerical probabilistic equations, they showed that their curves correspond to 50% of Saucedo's model curves [6].

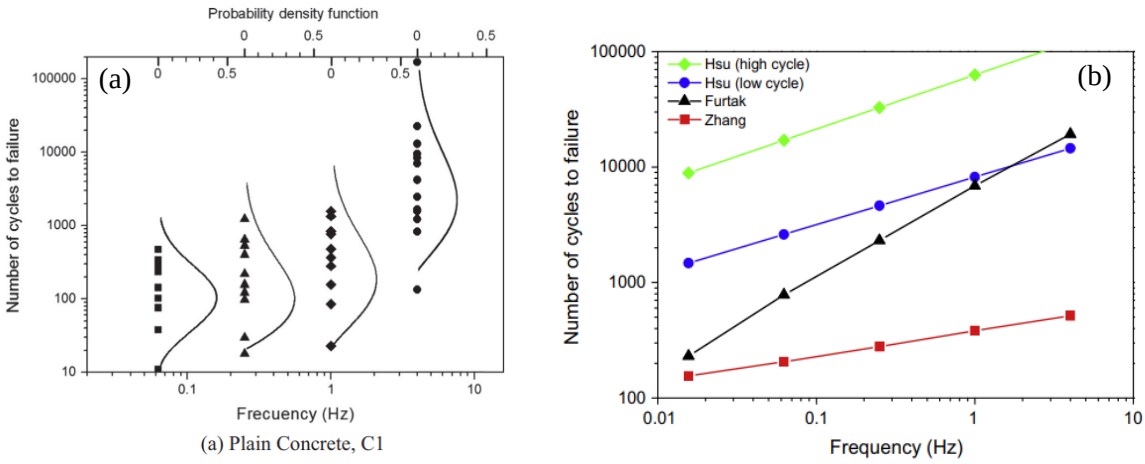

Fig. 15: (a) Number of cycles to failure versus loading frequency (Medeiros et al. [105]), (b) Number of cycles to failure versus frequency from three models (Medeiros et al. [105]).

Pavements are another kind of structure in which concrete is subjected to repeated loadings and fatigue, as in wind turbine foundations, and the fatigue knowledge obtained from papers from this other application can also be useful. Cervo and Balbo [102] studied the concrete fatigue for pavements and indicated that results from high frequencies (10 Hz) can overestimate the fatigue strength of concrete in lower frequencies. This is because the test with a high frequency seems to induce smaller crack openings inside the concrete, due to faster transient stress states, and, consequently, a lower progression of such cracks, resulting in a greater number of fatigue cycles at failure [117]. Similarly, this effect may exist in turbine foundations due to loadings associated to local wind frequency and intensity varying during the day and the year, as the other cited works confirm.

Fig. 16 is a graphical representation of the S-N curves of some studies. It is important to note that those tests were performed on samples with different dimensions and different compressive strengths. In comparison to these studies, the three common standards plus the Eq. (3) developed by [112] were also presented.

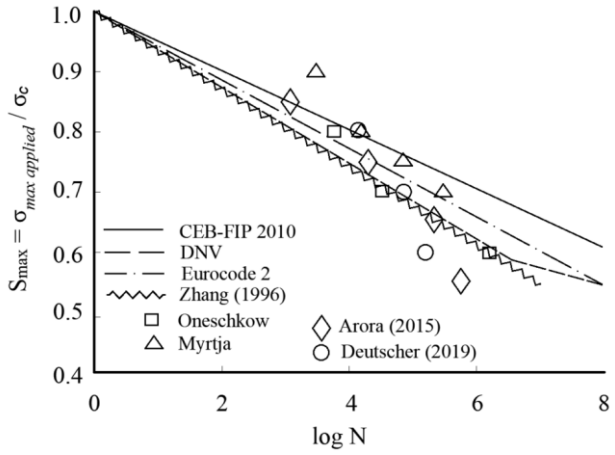

Fig. 16: Comparison of S-N curves of some recent studies for f = 10 (Hz).

Another point of interest has been considered by some researchers is the application of the resonance frequency of the specimen when dealing with fatigue tests. For this purpose, Thomas et al. [118] have applied cyclic compressive loads, with resonance frequency (very high frequency) and compared that to a uniform frequency of 10 Hz, to a high-strength plain concrete. The fatigue life of the specimen is lower when applying the resonant frequency. This higher frequency induces an increase in the temperature, which is due to the increase in creep damage. These results agreed with the results obtained by Sainz-Aja et al. [47] (their study was described previously in Section III.2). These studies have shown that the choice of the loading frequency to be applied, which is typically limited to about 15 Hz may be insufficient to evaluate concrete fatigue, because the fatigue life seems to be higher in this area and tends to drop towards much higher frequencies.

As previously explained, the high load rate application for high frequency, led to the formation of smaller crack openings for high stress levels (usually $S_{max} > 0.80$). Nevertheless, for low stress levels (usually $S_{max} < 0.80$), this behavior is not so pronounced, and it is slightly reversed for some study cases. This was explained by the temperature increase with the material fatigue, which is more pronounced for low stress levels and especially in high frequencies, decreasing the fatigue strength of the material.

From these observations, it should be quite necessary to consider and measure several parameters, when studying the fatigue behavior of materials. It is clear that more research is needed on this topic due to discrepancies, possibly due to lack of temperature control during tests and various temperature increases of specimens. The effect of temperature increase, which was induced in the study of loading frequency effects, appears to be very significant, especially when changing the stress level. Therefore, section IV.5 is dedicated to the presentation of the material heating during its fatigue.

IV.2. Environmental conditions

For structures in contact or immersed in water, such as onshore and offshore wind turbines, respectively, the moisture content of concrete - or grout - could have a significant effect on the fatigue life of the material. So, when studying the fatigue behavior, the environment in which the material is stored before and during the cyclic loading, has an important effect on its resistance to dynamic loads. In the DNV-OS-H101 [36] report, it has been noted that concrete is less supporting the dynamic loads when it is tested underwater than in the air. Despite the importance this factor could have, literature has not paid much attention to this effect. Here, we present, in detail, the few studies (on grout and concrete) that have considered the storage environment, as a parameter affecting fatigue life of material. It should be noted that the concrete compressive static strength is just slightly affected by the storage environment and moisture content [52,109].

Soerensen et al. [98] tested a high-performance grout used as connection of offshore wind turbine monopile (Fig. 6a), under cyclic compressive loading. This grout with a maximum diameter of the aggregate of 4 mm (natural sand), has a compressive strength of 170 MPa (the value noted at the

beginning of the fatigue tests, which were performed between 4 and 26 months before) obtained from compression tests done on cubic specimens of 100 mm. Two types of tests were investigated: (1) the specimen is kept in the air for the whole test; (2) the specimen is submerged in a reservoir saturated with water. All cylindrical samples tested under fatigue loads are 60-mm diameter by 120-mm height. Three frequencies are evaluated (0.35, 5 and 10 Hz) for three stress levels S_{max} (0.45, 0.60, and 0.76). For all tested frequencies, the number of cycles is reduced only in the wet environment. This phenomenon has been explained by a possible retention of water in the cracks developed during loads application. The decrease in fatigue life, for the wet environment is shown to be more significant for lower frequencies. This could be explained by the long duration of applied loads, which gives more time to water for its infiltration in cracks causing more damage.

Oneschkow et al. [26] studied the behavior of cylindrical concrete samples under two different environmental conditions: dry and wet. This means that the specimens were stored and tested in the same condition. After the storage, the moisture content was measured, showing that the wet specimens have about 20 kg/m^3 more moisture content than the dry ones. The tests were done on the specimens of 60-mm diameter by 120-mm height for two frequencies (1 and 10 Hz). They showed that the number of cycles to failure in the wet environment is lower than that of the dry environment, which is more significant for low loading frequency, and for low stress levels. Nygard et al. [119] studied the dynamic behavior of three types of concrete: normal strength concrete (NSC), high strength concrete (HSC), and lightweight concrete (LC), as well as two specimen sizes (50-mm diameter by 100-mm height). Their results indicated that the number of cycles underwater is significantly lower than under dry conditions. This was also observed earlier by [120,121], who tested the concrete specimens under alternating conditions between storage and the test itself. Ohlsson et al. [122] performed fatigue tests at 20ºC and -35ºC. They found that low temperatures increase, with frost, the fatigue strength for concrete with high moisture content. Authors suggested that was probably because of the ice formed that can carry some of the applied stress, working as an ice skeleton, contributing to the fatigue strength. However, it is emphasized here that they did not test how the fatigue strength would change after freeze-thaw cycles. Cervo and Balbo [102] studied the effect of saturation on the fatigue behavior of concrete. For the tested conditions, the number of cycles of saturated concrete was 1% to 19% of the fatigue strength of dry concrete for stress ratios below 0.95. Saturation was produced with 7 days immersion and kept during the test using soaked tissues in contact with the specimen. Some studies [123] have found no difference in fatigue behavior between concrete in dry conditions and concrete immersed in water. They tested two types of HSC: NC (normal-weight concrete) and LC (light-weight concrete), they just affirmed that life fatigue of LC was similar to or better than NC's one.

From all the discussed results, one could affirm that the capacity of the material to resist to fatigue loading decreases when the specimen is submerged in water during the test. The presence of water in the material can cause infiltrations in the microcracks and exert higher pressures, which can cause the

expansion of cracks and then a reduction of concrete's strength to fatigue. This phenomenon should be more pronounced at higher frequencies because of the rapidity of loading application, which leads to the rapid formation of microcracks. Whether it is concrete or grout, the effect of the test environment depends on the material performance and its characteristics. For high-performance materials, their more brittle character can have negative consequences on their fatigue resistance, since this characteristic offers an ease of cracking, permitting water to infiltrate easily, and thus form even more cracks.

To explain this phenomenon, on the one hand, by understanding physically how the introduction of water affects negatively the fatigue strength of the material, Tomann et al. [109] tried to understand how moisture content in microcracks induces low fatigue strength of concrete. They also used a multiscale numerical approach to describe damage mechanisms occurring when testing specimens in a wet environment. For this purpose, they tested cylindrical specimens of high-strength concrete HSC having dimensions of 100-mm diameter by 300-mm height. Five storage conditions: dried specimens at 105°C, natural conditions (20°C and 65% RH), intrinsic moisture (sealed until test), stored underwater. The specimens subjected to these four storage conditions are tested in air. A part of the specimens stored underwater is used for the fifth condition, for which tests are performed underwater [109]. Their results are also in accordance with the investigations mentioned above, showing a decrease of fatigue strength with an increase of moisture content of concrete. They performed other tests, to evaluate the frequency effect underwater, on specimens stored also underwater. The number of cycles to failure is increasing with frequency, showing that frequency strongly affects water-induced damage mechanisms, which are responsible for the fatigue strength decrease. To evaluate this damage mechanism, they calculated the gradient stiffness, and have followed the evolution of acoustic emission, which was considered as a damage indicator. Both show a high increase in moisture content (Fig. 17a), leading to low fatigue resistance. From their results, Tomann et al. [109] affirm, contrary to other investigations, that the moisture content is predominantly responsible for fatigue resistance decreasing, instead of the wet storage environment. They indicate a critical value of moisture content (3.5 mass-%), from which damage mechanisms due to water infiltration are induced.

On the other hand, Miura et al. [124] tried to examine the primary cracks developed in the presence of water, on static and fatigue behavior of concrete. As previously stated, we should remember that the decrease in the fatigue life and compressive strength of concrete is due to the micro-crack's propagation. As a result, Miura et al. [124] modified the existing model [125], which consists of estimating the compressive strength decrease function of the crack width (the cause of this reduction), and thus of the maximum aggregate size (these are directly related). The modification consists of the addition of a threshold value of the maximum average crack width, determined from the aggregate size. Based on results, they found that the reduction of fatigue life is independent of crack width.

Nevertheless, the crack width affects the second phase of the strain evolution, by accelerating the process of evolution.

To compare results for wet conditions for different studies, we present the S-N curves of materials tested underwater, for three loading frequencies (Fig. 17b) performed from different investigations. These curves were compared with the common standards. Thus, we observe that CEB-FIP Model [9] and Eurocode 2 [35] overestimate N*f* for wet environment, while DNV-OS-C502 [14] underestimates it. N*f* are similar for each frequency, and it increases with frequencies also in a wet environment. It should be noted that the test conditions (except for the environmental one) are not all the same for the authors.

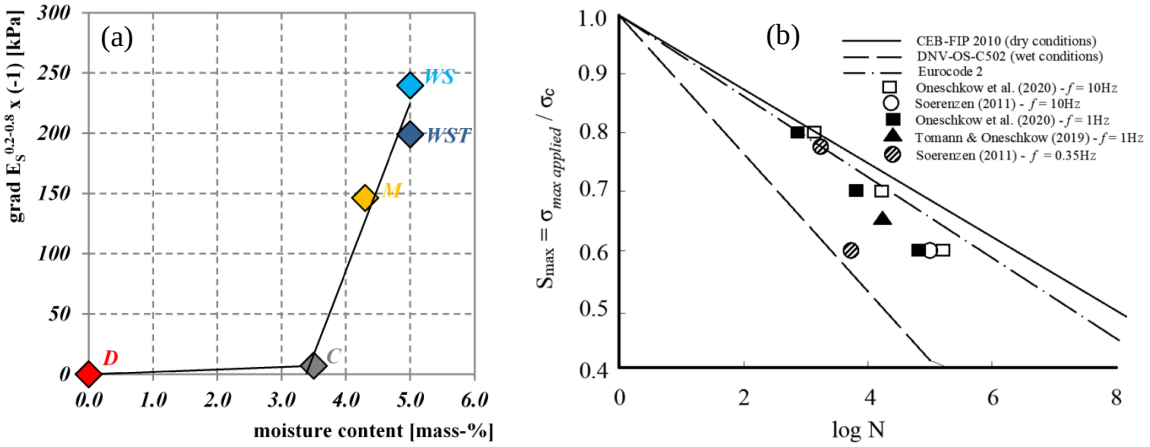

Fig. 17: (a) Gradient stiffness evolution with moisture content, (b) Comparison of S-N curves of some recent studies for wet conditions, for different loading frequencies.

IV.3. Specimen size

It is well known that the static compressive strength varies with the specimen size [126,127]. Some authors thought that this parameter would probably influence the dynamic behavior of the material as well. However, this parameter was not examined much for this subject. Nygard et al. [119] tested three types of concrete (NSC, HSC, and LC) for specimens with two different diameters 50 mm and 100 mm. For the tested concrete, they showed that by increasing the diameter of the specimen, the number of cycles increase. Oneschkow et al. [26] have evaluated this effect by testing two different sizes of sample: 60-mm diameter by 180-mm height and 100-mm diameter by 300-mm height, in dry conditions under the effect of two loading frequencies. They found that the number of cycles is lower for a high sample size (Fig. 18a). For S_{max} = 0.80, this difference in number of cycles, is more important for f = 10Hz than for f = 1Hz. Contradictory behavior for a wet environment compared to a dry environment, was observed for the loading frequency of f = 1 Hz and S_{max} < 0.80. This difference was reversed for S_{max} = 0.70. The same result was found by Thiele [128], and by Schneider et al. [129] who also tested specimens with 60-mm diameter by 180-mm height and 100-mm diameter by 300-mm height, varying the stress level and frequency. In addition, Thiele [128] shows that the number of

cycles to failure changes strongly despite a little change in the stress level. Bazant and Schell [126] tested three-point-bend notched beams of different depths 38, 107, and 304 mm in cyclic loading, for different stress levels. They adjusted the equation defining the cracks growth by adding the size effect.
The specimen size has also its effect on the temperature increase, affecting the fatigue life of the material. For this purpose, Hümme [130] tested specimens with 60-mm diameter by 180-mm height and 100-mm diameter by 300-mm height for 1 Hz and at a stress level of S_{max} = 0.7. The results showed that initially, the curves of the temperature increase (Fig. 18b) are similar for the two tested specimens but after a few hundred cycles, the curves of the temperature increase completely change their shapes and the maximum value stabilizes around 10 K, while for the higher size specimen, the temperature of the specimen keeps increasing rapidly and reach a value of approximately 16 K, that induces high fatigue life. The temperature increase for high size seems logical because the high dimension of the specimen offers a larger space for its heating due to fatigue.

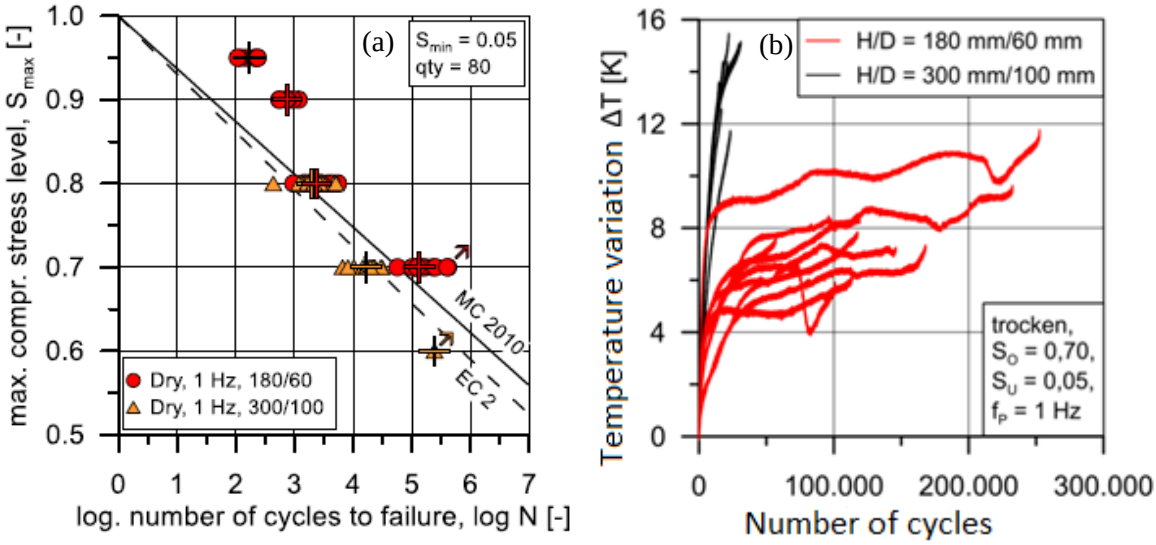

Fig. 18: (a) S-N curves affected by specimen size effect (Oneschkow et al. [26]), (b) Temperature increase due to the largest size of the specimen (Hümme [130]).

IV.4. Other parameters associated with the loading

This paragraph discusses other parameters that influence fatigue test results. Amongst them, we underline the one associated with the order of the loading when multiple loading levels are used; the one associated with rest periods between loadings; and the one associated with waveform.
Cervo and Balbo [102] analyzed the effect of stress variation (concerning the ratio S_{max} between the applied stress level and the one required to failure in one cycle – the static strength) during the cycles for concrete fatigue. The referred authors tested the following configurations of stress path: (i) constant stress levels during the cycles, with S_{max} = 0.83; (ii) increasing stress levels with S_{max} = 0.75

during 50000 cycles, then S_{max} = 0.79 during 30000 cycles, then S_{max} = 0.83 until failure; (iii) decreasing stress levels with S_{max} = 0.85 during 50000 cycles and S_{max} = 0.83 until failure. They found that the number of cycles obtained with decreasing stresses was lower than those obtained for constant or increasing stress. Baktheer and Chudoba [59] reviewed the concrete fatigue under compression considering the nonlinear effect of the loading sequence, to determine the remaining fatigue life of concrete. The referred authors focused on compressive cyclic loading with varying ranges. Authors observed that Miner's rule is insufficient to explain experimental observations and proposed an improved version of the damage accumulation hypothesis. Hilsdorf and Kesler [3] tested specimens with a range of age from 150 to 300 days at a speed of 450 cycles per minute and the ratio of the minimum to the maximum load was 0.17 for all tests. The fatigue machine was stopped for a rest period of 1, 5, 10, 20, or 27 minutes after 4500 load cycles, when the specimen was subjected to a constant load equivalent to the lower limit of the load cycles, which was considered the rest. This procedure was repeated until failure. The referred authors discovered that rest periods between load cycles increases the fatigue life of concrete. Up to five-minute breaks between each load sequence can extend the lifetime. Rest periods longer than five minutes did not seem to extend the fatigue life further. Authors concluded that Miner's rule hypothesis may diverge from actual behavior depending on the load program.

Tepfers et al. [131] tested how fatigue strength is affected by applying the load in different waveforms: Sinusoidal, triangular and rectangular. They found that the specimen cracked with less cycles with the rectangular waveform, which is reasonable since the specimen is subjected to higher stresses over a longer period compared to other forms. According to Tepfers [131], the influence of the three fatigue loading waveform types were illustrated. Different shapes of failure are observed, depending on the waveform applied (Fig. 19). As shown in the figure, when applying rectangular waveform loading, failure by fatigue occurs rapidly. It is also shown that the sinusoidal waveform required the highest N*f*. In a recent study, Oneschkow [72] confirmed that by comparing triangular and sinusoidal waveforms applied on HSC, for two frequencies (0.89 and 1 Hz) and two stress levels (0.80 and 0.90).

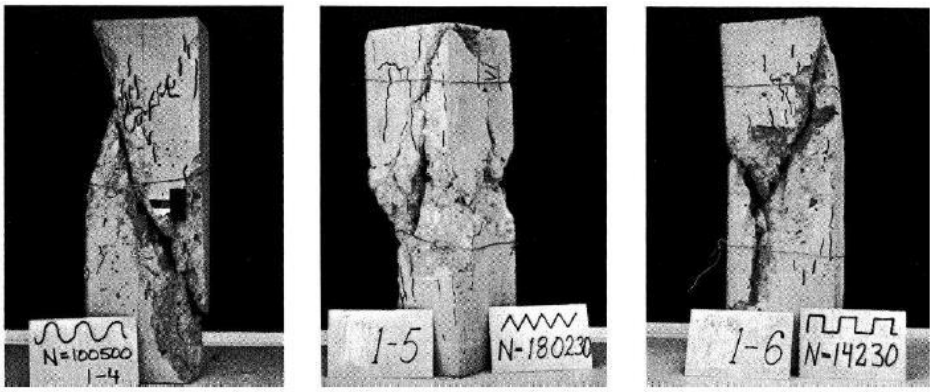

Fig. 19: Different shapes of failure from Tepfers et al. [131], for three types of applied cyclic loading respectively: sinusoidal, triangular, and rectangular.

Saini and Singh [132] performed flexural fatigue strength tests of self-compacting concrete made with recycled concrete aggregates and mixed cements. For the fatigue test, 224 beams with dimensions of 100 x 100 x 500 mm^3 were tested, using stress levels ranging from 0.95 to 0.65 and a constant stress ratio equal to 0.1. The tests were performed at a frequency of 10 Hz, with a sine wave signal. The criteria for stopping the tests were when a material failure was reached or when the number of cycles was equal to 2 million. The data obtained in each test were represented in the S-N curve. Data showed convincing scatter in fatigue life, requiring the establishment of fatigue resistance probabilistic models. There was a reduction in the compressive and flexural strength with the addition of recycled aggregate, which could later be compensated with the addition of cement with metakaolin and silica fume. In the same context of studies concerning the incorporation of mineral additives in concrete, Golewski [133] have studied the effect of the fly ash (FA) addition (20% and 30%) on the fracture toughness of concrete, by considering the three cracking models. He concluded that the addition of 20% FA is the most advantageous, offering higher mechanical parameters, and higher fracture toughness of the material. Furthermore, Gil and Golewski [134] have done the same study but with one more addition only for the first model of cracks, and for the addition of FA and Silica Fume (SF). The best results were obtained for a combined addition of 10% SF and 10% FA. This addition highly affects fracture mechanisms.

Vicente et al. [135] have studied the effect of the pore morphology in porous concretes subjected to compression cyclic loads on their fatigue lives. By developing a correlation between the porosity and the number of cycles to failure, they concluded that the fatigue life decreases by increasing porosity. However, they also showed that the presence of very small pores could induce a better behavior of concrete, depending on the pore size.

To evaluate the effect of alternating tensile and compression stresses, Cornelissen [103] performed concentric tensile and flexural tensile fatigue tests, compared to alternate tension-compression tests, on plain concrete. The results showed that the alternation of stress (tension-compression) highly reduces the fatigue life of concrete. In addition, it was also tested the effect of the environmental conditions, for which it was found that for wet specimens, the number of cycles decrease compared to dry specimens.

Morris and Garrett [136] also tested the effect of adding steel fibers to cement mortar, under static and dynamic loading in compression and tension. For both kinds of loading, it has been shown that fibers play a significant role in retarding the crack's initiation and propagation. Improvement in fatigue life is also noted for tests with a higher number of cycles. The effect of adding silica fume to HSC with LC and NC's types was also studied [123], showing an increase in the fatigue life of LC. No significant effect was found for this addition for NC. According to the authors, it is due to the improvement in the bond relating to concrete and its reinforcement.

To evaluate the behavior of concrete submitted to coupled 3D fatigue-static loading, Yang et al. [137] have performed fatigue tests using the triaxial compression dynamic-static tool. They characterize the relevant post-fatigue parameters of High-Strength Concrete (HSC), starting with those related to (1) wave propagation (longitudinal and transversal waves velocities), for which a delay has been noted, up to (2) the mechanical parameters (triaxial compressive strength, elastic modulus), showing a decreasing in their performances, and finally (3) the physical characteristics (porosity, permeability), for which an increase has been observed. Yang et al. [137] have also established an empirical prediction model based on the parameters affecting the fatigue (some of them are notably described in our paper) such as axial static stress, loading frequency, force amplitude, cycle number and confining stress, in order to establish a relation between these all parameters. From their results, they showed that the damage is more influenced by the axial loads compared to confining stress. In addition, they claim the existence of a threshold of stress, from which the physical and mechanical properties of HSC are directly decreased. They explain that by the crack growth, which highly increases the energy dissipation from a stress level S_{max} = 0.80 (Fig. 20a). They also showed two behaviors of the HSC depending on the number of cycles. For low-cycle fatigue, due to the randomly distribution of the crack's growth, a nonlinear behavior is observed while, at high-cycle fatigue, a linear behavior is noted, which is probably due to the stabilization of the crack's growth (Fig. 20b). Thus, they established correlation between damage variable and fatigue parameters.

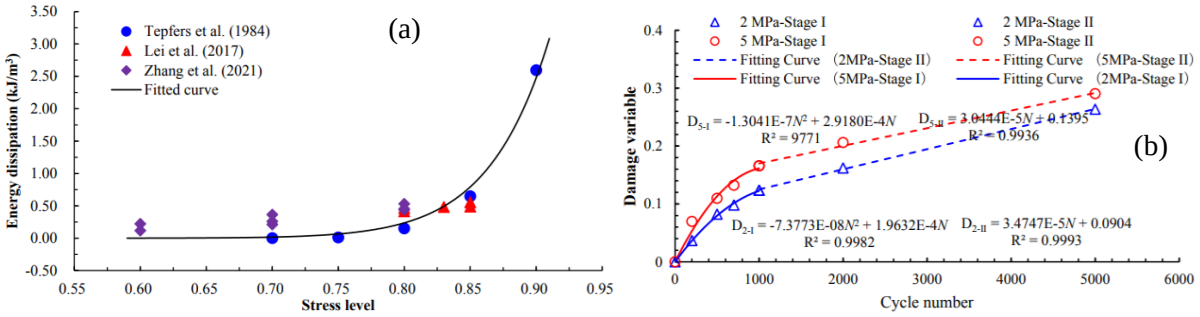

Fig. 20: (a) Single-cycle energy dissipation vs. stress level, (b) Damage variable vs. Cycle number (Yang et al. [137]).

IV.5. Temperature increase due to self-heating

As suggested by works discussed in the previous sections, the temperature increase has an impact on the fatigue life of materials. This was indirectly introduced when presenting the effect of the other parameters e.g., the frequency (cf. Section IV.1) and the specimen size effect (cf. Section IV.3).

Deutscher et al. [137] evaluated the effect of temperature increase due to the dynamic testing on the behavior of ultra-high-performance concrete (UHPC). They investigated the loading frequency (3, 10, and 20 Hz), the maximum grain size, and the maximum stress level. The minimum stress level (S_{min}) had a constant value of 10% for the whole test. Two UHPC were studied having the same strength but

different maximum grain sizes. The specimens used for this study have 60-mm diameter by 180-mm height dimensions. The tested concrete has a mean static strength of 160 MPa. During the test, the temperature was recorded on four points of the specimen: top, middle, bottom, and in the middle inside. An increase in the temperature was observed (Fig. 21a) for all the points with the number of cycles, with a higher temperature value in the middle (maximum temperature increase on the surface in top and bottom was approximately 13 K, on the surface in center 35 K, and in the center of the specimen 48 K), which means that the heating due to the fatigue loading is more concentrated in the middle of the specimens, and clearly inside.

Myrtja et al. [5] tested grout under dynamic loading using thermocouples to measure temperature during the tests. The intention is to measure the temperature increase in the middle of the specimen. Thermocouples were placed there. In order to obtain only the referred temperature increase, the temperature increase of the plates is subtracted from the temperature increase of the thermocouple. For f = 10 Hz, the maximum mean values of temperature rise are 28, 21 and 9 K for S_{max} = 0.75, 0.80 and 0.90 respectively (Fig. 21b). The authors compared their results to Elsmeier et al. [139], who tested this effect on a material with 2 mm maximum grain size, and which reach a value of 45 K for S_{max} = 0.60 for 59000 cycles. At this number of cycles approximately, Myrtja et al. [5] obtained about 30 K of temperature increase. The observed difference is probably due to the maximum grain size used in this study which is 6 mm, and possibly also environmental conditions. From this, it was assumed that the temperature rise occurs more in a material with small maximum grain size. However, one should note that also the difference between the materials used (nature of the aggregates, mechanical properties etc.) could be the reason behind the difference noted between the values. It should be observed that, in other materials, it has already been demonstrated from modelling and experiments that the temperature increase is due to viscous or to plastic dissipation during loading cycles [54,140]. In order to do the same for concrete, constitutive models including dissipative mechanisms should be fitted to concrete behavior prior to heat dissipation calculation. This could be the path to relate the measured temperature increase to the measured mechanical properties.

The comparison of the temperature increases between two frequencies (1 and 10 Hz) for S_{max} = 0.80, was also done by Myrtja et al. [5], who obtained a significant difference of the mean of the maximum values (about 15 K more for the higher frequency). The application of high loading rate at low frequency does not allow generating a high temperature (environment heat exchange predominates), contrary to a high frequency loading which allows a sufficiently fast loading ensuring a continuous development of the sample's heating. The authors also tested the effect of varying the stress level on the temperature increase (Fig. 21b). A low S_{max} lead to higher temperature. Fig. 21a illustrates temperature increase, experimentally observed for different positions [138] within the specimen, which show a high value of temperature increase in the middle of the specimen.

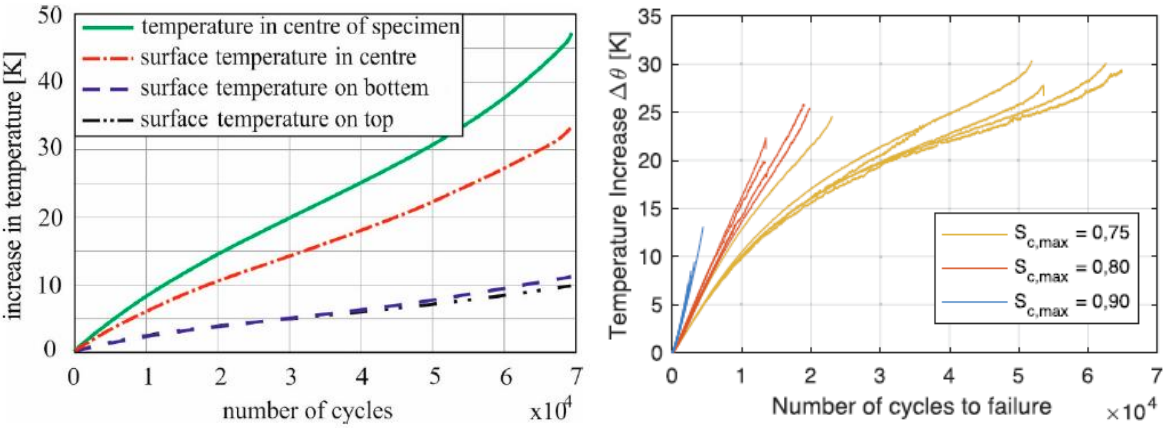

Fig. 21: Temperature increase (a) at different positions (Deutscher et al. [138]), (b) at different stress levels (Myrtja et al., 2021a), for f = 10 (Hz).

V. Synthesis

Table 2, below, presents a synthesis of the referred works cited previously. It may help the reader find rapidly the main information for each investigated topic.

Table 2: Synthesis of the investigated works

Frequency effect on fatigue life of concrete or grout		
References	**Comments**	**Conclusions**
Graf and Brenner [21]	First evaluation of the frequency effect	Effect of frequency was not very significant on fatigue
Awad and Hilsdorf [100]; Sparks and Menzies [101]	First consideration of the frequency as an influencing parameter on fatigue behavior of materials	Frequency started being considered a relevant parameter for fatigue
Cornelissen [103]; Zhang et al. [141]	Fatigue by tension and by bending on concrete varying frequency	High frequency → high N*f*
Zhang et al. [141]	Fatigue by bending on concrete varying frequency	Consideration of the frequency in the fatigue equation
Hümme et al. [52]; Medeiros et al. [105]; Oneschkow [114]; Saucedo et al. [6]; Sparks and Menzies [101]; Tomann et al. [109]; Oneschkow [72]; Weigler and Freitag [111]	Fatigue by pure compression tests varying frequency	High frequency → high N*f*
The combined effect of the frequency with the maximum stress levels S_{max}		
References	**Comments**	**Conclusion**
Naik et al. [106]; Raithby and Galloway [108]; Sparks and	First studies on concrete	

Menzies [101]		High frequency & low S_{max} → low N*f*
Hümme et al. [52]; Oneschkow [72]; Von der Haar and Marx [110]	Studies on concrete	
Otto et al. [107]	Studies on grout	
Hanson et al. [104]; Murdock [97]	Studies for $S_{max} < 0.75$, and for frequencies between 1 and 15 Hz	Insignificant effect of frequency
Sparks and Menzies [101]	Pure compression fatigue tests on concrete	High frequency & high S_{max} → frequency greatly affects N High frequency & low Smax → little effect of frequency
Cervo and Balbo [102]	Concrete fatigue for pavements	High frequency & low S_{max} → low N*f* High frequency & high Smax → high N*f*
Myrtja et al. [5]; Oneschkow et al. [26]	Fatigue for grout Fatigue for concrete	
Effect of environmental conditions		
References	**Comments**	**Conclusion**
Muguruma [120]; Muguruma and Watanabe [121]	Studied different conditions during storage and during the test itself	Wet conditions → low N*f*
Ohlsson et al. [122]	Fatigue tests at 20ºC and -35ºC.	Low temperatures with frost, with high moisture content → high N*f*
Mor et al. [123]	High-Strength Concrete: Normal-weigth Concrete and Light-weigth Concrete	No effect of wet conditions compared to dry conditions
Nygard et al. [119]	Pure compressive fatigue loading on NSC, HSC, and LC	Wet conditions → low N*f*
Cervo and Balbo [102]	Effect of saturation on the fatigue behavior of concrete	Saturated concrete had 1% to 19% of the fatigue strength of dry concrete
Soerensen et al. [98]	Effect of saturation on the fatigue behavior of concrete	Wet conditions → low N*f*
Tomann et al. [109]	5 conditions: dried specimens at 105°C, natural conditions (20°C and 65% RH), intrinsic moisture (sealed until test), stored underwater.	High moisture content → low N*f*. Frequency strongly affects water-induced damage mechanisms
Oneschkow et al. [26]	Pure compressive fatigue loading on HSC	The maximal difference between log N in dry conditions and wet

		conditions is approximately 1.5 powers of ten.
Effect of specimen size		
References	**Comments**	**Conclusion**
Nygard et al. [119]	Three types of concrete (NSC, HSC, and LC) tested, for two diameters 50 mm and 100 mm	Higher Diameter → higher N*f*
Bazant and Schell [126]	Three-point-bend notched beams tested of different depths 38, 107, and 304 mm	Adjusting the equation defining the cracks growth by adding the size effect
Thiele [128]; Schneider et al. [129]	Two dimensions tested: 60mm-D x 180mm-H and 100mm-D x 300mm-H	Higher Diameter → higher N*f* N*f* changes strongly despite a little change in the stress level
Hümme [130]	60mm-D x 180mm-H and 100mm-D x 300mm-H	After a few hundred cycles, the curves of the temperature increase change completely their shapes: Lower Diameter → 10 K Higher Diameter → 16 K → N*f*
Oneschkow et al. [26]	Two dimensions tested: 60mm-D x 180mm-H and 100mm-D x 300mm-H	Higher Diameter → higher N*f* the high difference is marked for higher frequency
Effect of other parameters associated with the loading		
References	**Comments**	**Conclusion**
Hilsdorf and Kesler [3]	Specimens with a range of age from 150 to 300 days The fatigue machine was stopped for a rest period of 1, 5, 10, 20, or 27 minutes after 4500 load cycles	The rest periods between load cycles increases the fatigue life of concrete.
Tepfers et al. [131]	Application of the load in different waveforms: Sinusoidal, triangular and rectangular	Rectangular waveform required a smaller number of cycles
Morris and Garrett [136]	The effect of adding steel fibers to cement mortar under static and dynamic loading in compression and tension	Fibers play a significant role in retarding the crack's initiation and propagation
Cornelissen [103]	The effect of alternating tensile and compression stresses	The alternation of stress (tension-compression) highly reduces the fatigue life of concrete
Mor et al. [123]	The effect of adding silica fume to	An increase in the fatigue life of

	HSC with LC and NC's types	LC. No significant effect for this addition for NC
Cervo and Balbo [102]	Stress variation (concerning the ratio R between the applied stress level and the one required to failure in one cycle – the static strength	N*f* obtained with decreasing stresses was lower than those obtained for constant or increasing stress
Vicente et al. [142]	Effect of the pore morphology in porous concretes subjected to compression cyclic loads	Fatigue life decreases by increasing porosity
Baktheer A, Chudoba R [59]	Consideration of the nonlinear effect of the loading sequence under compression	Miner's rule is insufficient to explain experimental observations Proposition of an improved version of the damage accumulation hypothesis
Saini and Singh [132]	Flexural fatigue tests of self-compacting concrete made with recycled concrete aggregates and mixed cements.	Data showed convincing scatter in fatigue life. There was a reduction in the compressive and flexural strength with the addition of recycled aggregate.
Effect of temperature increase due to self-heating		
References	**Comments**	**Conclusion**
Deutscher et al. [138]	Cyclic testing on the behavior of ultra-high-performance concrete (UHPC).	Heating due to the fatigue loading is more concentrated in the middle and inside the specimens.
Elsmeier et al. [139]	2 mm maximum grain size	ΔT = 45 K for S_{max} = 0.60 for 59000 cycles
Myrtja et al. [143]	Comparison with Elsmeier et al. [139]. 6 mm maximum grain size	ΔT = 30 K of temperature increase for 59000 cycles. Temperature rise occurs more in a material with small maximum grain size

VI. Recommendations for future research

Some gaps are observed in this review, particularly with respect to:

(i) comprehensive loading configurations (using both compression and tension in tests).

(ii) temperature increase interpretation and effects on fatigue: from the analysis in this paper, the temperature was found to be a very important for fatigue. It is therefore strongly recommended to deeply investigate the temperature increase in tests and its effects on fatigue test results.

(iii) parameters dependence: from results recorded, it was shown that the main parameters affecting fatigue life of concrete are interdependent, which highly complicates the comprehension of the fatigue mechanisms. One proposition to deal with that, is to do a complete study which could consider, as much as possible, several parameters at once. It would be a solution to avoid some higher variation of results noted, in some studies, for specimens with the same properties.

(iv) modulus tracking during tests and how to include resulting information in fatigue prediction models: because of the difficulty of performing fatigue tests regarding time-consumption, necessity of materials and the variability of the results, it is suggested to develop the existing prediction models.

Authors hope these aspects may be object of research projects in the near future.

VII. Conclusions

This paper presented an overview of fatigue characterization procedures for concrete and investigated the available literature with respect to different aspects of concrete fatigue, particularly: (i) effect of loading frequency; (ii) effect of environmental conditions (temperature and moisture); (iii) size effect; (iv) other effects such as the relevance of the order of the employed loading amplitudes (nonlinearity with respect to Miner's equation); (v) self-heating of concrete specimens during fatigue tests. It contributes with the organization of the body of knowledge and the establishment of some open questions in the literature. There are still many aspects of concrete fatigue behavior without consensus in the literature, particularly on temperature and frequency effects and self-heating of specimens during tests. It is clear that it is necessary to continue developing and improving methods to characterize and interpret concrete fatigue in order to allow in the future better design of structures subjected to fatigue, e.g. wind tower concrete foundations. Some key conclusions can be summarized as follows:

- Comparing different standards, regarding concrete fatigue, there is a considerable variation between them, depending on the code applied. For instance, comparing considerations between all cited standards [9,35,36], it is shown that the Norwegian code [36] underestimates the fatigue life in comparison to others;

- The specimen dimensions are relevant for temperature increase, which is expected due to a larger volume to the self-heating effect. The loading frequency also plays a role in the

temperature increase, with higher frequency leading to more temperature increase (there is more energy dissipation in less time). Temperature has relevant impact on fatigue life. Then, it can be seen as an artifact and biasing effect that requires further investigation in the future. Energy dissipation from inelastic phenomena during the loading cycles may be related to the temperature increase, as already investigated for other materials. This could be the path to correct temperature effects from the interpretations of accelerated fatigue lab tests results and use corrected data for field prediction;

- Although consensus is not observed in the literature (possibly due to a combined effect with the temperature increase, which is not always measured), it appears that loading frequency influences fatigue, which is a particularly relevant concern, since tests in laboratory need to be accelerated (high frequency) compared to the field (low frequency);

- When it comes to the loading waveform shapes, it was found that a rectangular shape provides a shorter fatigue life, compared to all others, particularly the sinusoidal shape. This is also expected to the time of higher loading actually applied;

- Alternated compression and tensile stresses highly reduce the fatigue life, and literature misses more comprehensive evaluation of the effect of loading (either in tension, in compression, or in tension-compression);

- Concerning the environmental conditions, despite the fact that moisture content during storage and during tests rather slightly affects the compressive strength, they significantly decrease fatigue life;

- Steel fibers play a significant role in retarding the cracks initiation and its coalescence to macrocracks;

- The addition of silica fumes increases the fatigue life, which is possibly related to a porosity decrease. Porosity influence on fatigue is also a matter that could be further investigated;

- It was also demonstrated that many fatigue damage models available in the literature may be used to adequately represent the measured properties of concrete during fatigue tests. There seems to be room to include them in future fatigue calculation procedures.

Funding sources

We thank the European Regional Development Fund (Fonds Européen de Développement Régional, FEDER) for having sponsored this study in the frame of the FONDEOL project N° 19P03379 – 19E00936.

Acknowledgment

We thank Daniel Lira from *Universidade Federal do Ceará* for proof-reading the full paper and suggested modifications for clarity's sake.

References

[1] Hordijk DA. Local approach to fatigue of concrete. 1993:1.
[2] Aas-Jakobsen K. Fatigue of concrete beams and columns. Trondheim: [Tapir]; 1970.
[3] Hilsdorf HK, Kesler- CE. Fatigue Strength of Concrete Under Varying Flexural Stresses. JP 1966;63:1059–76. https://doi.org/10.14359/7662.
[4] Lee MK, Barr BIG. An overview of the fatigue behaviour of plain and fibre reinforced concrete. Cement and Concrete Composites 2004;26:299–305. https://doi.org/10.1016/S0958-9465(02)00139-7.
[5] Myrtja E, Soudier J, Prat E, Chaouche M. Fatigue deterioration mechanisms of high-strength grout in compression. Construction and Building Materials 2021;270:121387. https://doi.org/10.1016/j.conbuildmat.2020.121387.
[6] Saucedo L, Yu RC, Medeiros A, Zhang X, Ruiz G. A probabilistic fatigue model based on the initial distribution to consider frequency effect in plain and fiber reinforced concrete. International Journal of Fatigue 2013;48:308–18. https://doi.org/10.1016/j.ijfatigue.2012.11.013.
[7] Lemaitre J, Chaboche J-L. Mechanics of Solid Materials. Cambridge: Cambridge University Press; 1990. https://doi.org/10.1017/CBO9781139167970.
[8] Pastoukhov, Voorwald. Introdução à mecânica da integridade estrutural. Editora Unesp 1995. http://editoraunesp.com.br/catalogo/8571390800,introducao-a-mecanica-da-integridade-estrutural (accessed August 24, 2021).
[9] CEB-FIP Model. CEB Bulletins : CEB-FIP Model Code 90 (PDF) 1990. https://www.fib-international.org/publications/ceb-bulletins/ceb-fip-model-code-90-pdf-detail.html (accessed August 24, 2021).
[10] DNV-OS-J101. Design of Offshore Wind Turbine Structures 2004:138.
[11] Wang X, Fang S. Comparison of Fatigue Design Code Requirements for Wind Turbine Foundations. SP 2021;348:145–58.
[12] Viswanath S, Kuchma DA, LaFave JM. Experimental Investigation of Concrete Fatigue in Axial Compression. SJ 2021;118:263–76. https://doi.org/10.14359/51728185.
[13] Brebbia CA, Walker S. Dynamic Analysis of Offshore Structures. Newnes; 2013.
[14] DNV-OS-C502. DNV-OS-C502: Offshore Concrete Structures 2010:102.
[15] Golewski GL. On the special construction and materials conditions reducing the negative impact of vibrations on concrete structures. Materials Today: Proceedings 2021;45:4344–8. https://doi.org/10.1016/j.matpr.2021.01.031.
[16] Considere M. Influence of rebar on the properties of mortars and concretes (Influence dês armatures métalliques sur lés propriétés dês mortiers et bétons). Compte Redu de L'Academic Des Sciences 1899;127:992–5.
[17] Joly, D. La resistance et l,'"elasticite des"'ciments Portland 1898.
[18] Ornum JLV. The Fatigue of Cement Products. Transactions of the American Society of Civil Engineers 1903;51:443–5. https://doi.org/10.1061/TACEAT.0001612.
[19] Clemmer HF. Fatigue of concrete. Proceedings, ASTM, vol. 22, 1922, p. 408–17.
[20] Hatt WK. FATIGUE OF CONCRETE. Highway Research Board Proceedings 1925;4.
[21] Graf O, Brenner E. Versuche zur Ermittlung der Widerstandsfähigkeit von Beton gegen oftmals wiederholte Druckbelastung. Mitteilungen Der Deutschen Materialprüfungsanstalten 1940:416.

[22] Aas-Jakobsen K, Lenschow R. Behavior of Reinforced Columns Subjected to Fatigue Loading 1973. https://www.concrete.org/publications/internationalconcreteabstractsportal.aspx?m=details&ID=11198&m=details&ID=11198 (accessed August 25, 2021).
[23] Tepfers R, Kutti T. Fatigue strength of plain, ordinary and lightweight concrete. Journal of the American Concrete Institute 1979;76:635–52.
[24] Furtak K. Ein verfahren zur berechnung der betonfestigkeit unter schwellenden belastungen. Cement and Concrete Research 1984;14:855–65. https://doi.org/10.1016/0008-8846(84)90012-7.
[25] Wöhler A. Über die Festigkeitsversuche mit Eisen und Stahl. Ernst & Korn; 1870.
[26] Oneschkow N, Hümme J, Lohaus L. Compressive fatigue behaviour of high-strength concrete in a dry and wet environment. Construction and Building Materials 2020;262:119700. https://doi.org/10.1016/j.conbuildmat.2020.119700.
[27] Van Eck NJ, Waltman L. VOSviewer manual. Leiden: Univeristeit Leiden 2013;1:1–53.
[28] Korte S. Experimental and numerical investigation of the fracture behaviour and fatigue resistance of self-compacting concrete. dissertation. Ghent University, 2014. https://doi.org/10/file/5912751.
[29] A03-406 1993. https://www.boutique.afnor.org/norme/a03-406/produits-metalliques-fatigue-sous-sollicitations-d-amplitude-variable-methode-rainflow-de-comptage-des-cycles/article/684090/fa029290 (accessed August 24, 2021).
[30] ASTM E1049 - 85. Standard Practices for Cycle Counting in Fatigue Analysis 2017. https://www.astm.org/Standards/E1049.htm (accessed August 24, 2021).
[31] SOLCYP. Structure des Recommandations 2017:24.
[32] Downing SD, Socie DF. Simple rainflow counting algorithms. International Journal of Fatigue 1982;4:31–40. https://doi.org/10.1016/0142-1123(82)90018-4.
[33] Miner MA. Miner, M.A. (1945) Cumulative Damage in Fatigue. Journal of Applied Mechanics, 3, 159-164. - References - Scientific Research Publishing 1945. https://www.scirp.org/(S(351jmbntvnsjt1aadkposzje))/reference/ReferencesPapers.aspx?ReferenceID=1754154 (accessed August 24, 2021).
[34] ACI PRC-215-92. ACI PRC-215-92: Considerations for Design of Concrete Structures Subjected to Fatigue Loading (Reapproved 1997) 1997. https://www.concrete.org/store/productdetail.aspx?ItemID=21592&Format=DOWNLOAD&Language=English&Units=US_AND_METRIC (accessed August 25, 2021).
[35] Eurocode 2. AFNOR, NF EN 1992 Partie 2 : Ponts en béton — Calcul et dispositions constructives, LCP-Con. (2006) - Recherche Google 1992. https://www.google.com/search?q=AFNOR%2C+NF+EN+1992+Partie+2+%3A+Ponts+en+b%C3%A9ton+%E2%80%94+Calcul+et+dispositions+constructives%2C+LCP-Con.+(2006)&rlz=1C1CHBD_frFR935FR935&oq=AFNOR%2C+NF+EN+1992+Partie+2+%3A+Ponts+en+b%C3%A9ton+%E2%80%94+Calcul+et+dispositions+constructives%2C+LCP-Con.+(2006)&aqs=chrome..69i57.327j0j7&sourceid=chrome&ie=UTF-8 (accessed October 8, 2021).
[36] DNV-OS-H101. DNV-OS-H101: Marine Operations, General 2011:55.
[37] Model Code 2010. Model Code 2010. Structural Concrete 2013;14:230–41. https://doi.org/10.1002/suco.201300003.
[38] ABNT NBR 6118. ABNT Catalogo 2014. https://www.abntcatalogo.com.br/norma.aspx?ID=317027 (accessed August 25, 2021).

[39] Golewski GL. The Specificity of Shaping and Execution of Monolithic Pocket Foundations (PF) in Hall Buildings. Buildings 2022;12:192. https://doi.org/10.3390/buildings12020192.
[40] Golewski GL. new principles for implementation and operation of foundations for machines: A review of recent advances. 1 2019;71:317–27.
[41] Børsheim H. Concrete fatigue of onshore wind turbine foundations 2020.
[42] NS-EN 1992-1-1. NS-EN 1992-1-1:2004+NA:2008 2004. https://www.standard.no/no/nettbutikk/produktkatalogen/produktpresentasjon/?ProductID=353701 (accessed August 25, 2021).
[43] Det Norske Veritas. Summary report from JIP on the capacity of grouted connections in offshore wind turbine structures. Norway: Det Norske Veritas 2010.
[44] Balbo JT. Fatos, mitos e falácias sobre os modelos experimentais de fadiga. Reunião Anual de Pavimentação 2000;1:391–404.
[45] Hsu. Fatigue of Plain Concrete. ACI Journal Proceedings, 78, 292-305. - References - Scientific Research Publishing 1981. https://www.scirp.org/(S(i43dyn45teexjx455qlt3d2q))/reference/ReferencesPapers.aspx?ReferenceID=1403894 (accessed September 21, 2021).
[46] Paskova T, Meyer C. Optimum Number of Specimens for Low- Cycle Fatigue Tests of Concrete. Journal of Structural Engineering 1994;120:2242–7. https://doi.org/10.1061/(ASCE)0733-9445(1994)120:7(2242).
[47] Sainz-Aja J, Thomas C, Carrascal I, Polanco JA, de Brito J. Fast fatigue method for self-compacting recycled aggregate concrete characterization. Journal of Cleaner Production 2020;277:123263. https://doi.org/10.1016/j.jclepro.2020.123263.
[48] Locati L. Le prove di fatica come ausilio alla progettazione ed alla produzione. Metallurgia Italiana 1955;47:301–8.
[49] Sainz-Aja J, Thomas C, Polanco JA, Carrascal I. High-Frequency Fatigue Testing of Recycled Aggregate Concrete. Applied Sciences 2020;10:10. https://doi.org/10.3390/app10010010.
[50] Isojeh B, El-Zeghayar M, Vecchio FJ. Concrete Damage under Fatigue Loading in Uniaxial Compression. ACI Materials Journal 2017;114. https://doi.org/10.14359/51689477.
[51] Di Benedetto H, de La Roche C, Baaj H, Pronk A, Lundström R. Fatigue of bituminous mixtures. Mat Struct 2004;37:202–16. https://doi.org/10.1007/BF02481620.
[52] Hümme J, Haar C von der, Lohaus L, Marx S. Fatigue behaviour of a normal-strength concrete – number of cycles to failure and strain development. Structural Concrete 2016;17:637–45. https://doi.org/10.1002/suco.201500139.
[53] Balit Y, Joly L-R, Szmytka F, Durbecq S, Charkaluk E, Constantinescu A. Self-heating behavior during cyclic loadings of 316L stainless steel specimens manufactured or repaired by Directed Energy Deposition. Materials Science and Engineering: A 2020;786:139476. https://doi.org/10.1016/j.msea.2020.139476.
[54] Babadopulos LF, Sauzéat C, Di Benedetto H. Thermomechanical Coupling in Bituminous Mixtures Considered as Bonded Granular Media 2017:610–7. https://doi.org/10.1061/9780784480779.075.
[55] Holmen JO. Fatigue of concrete by constant and variable amplitude loading. Trondheim, Norway: Division on Concrete Structures, Norwegian Institute of Technology, University of Trondheim; 1979.
[56] Viswanath S, LaFave JM, Kuchma DA. Concrete compressive strain behavior and magnitudes under uniaxial fatigue loading. Construction and Building Materials 2021;296:123718. https://doi.org/10.1016/j.conbuildmat.2021.123718.

[57] Park YJ. Fatigue of Concrete under Random Loadings. Journal of Structural Engineering 1990;116:3228–35. https://doi.org/10.1061/(ASCE)0733-9445(1990)116:11(3228).
[58] Isojeh B, El-Zeghayar M, Vecchio FJ. Simplified constitutive model for fatigue behavior of concrete in compression. Journal of Materials in Civil Engineering 2017;29:04017028.
[59] Baktheer A, Chudoba R. Enhanced assessment rule for concrete fatigue under compression considering the nonlinear effect of loading sequence. International Journal of Fatigue 2019;126:130–42.
[60] Chaboche JL, Lesne PM. A non-linear continuous fatigue damage model. Fatigue & Fracture of Engineering Materials & Structures 1988;11:1–17.
[61] Fathima KP, Kishen JC. A thermodynamic framework for the evolution of damage in concrete under fatigue. Archive of Applied Mechanics 2015;85:921–36.
[62] Huang B-T, Li Q-H, Xu S-L. Fatigue deformation model of plain and fiber-reinforced concrete based on Weibull function. Journal of Structural Engineering 2019;145:04018234.
[63] Keerthana K, Kishen JC. An experimental and analytical study on fatigue damage in concrete under variable amplitude loading. International Journal of Fatigue 2018;111:278–88.
[64] Liu F, Zhou J. Fatigue strain and damage analysis of concrete in reinforced concrete beams under constant amplitude fatigue loading. Shock and Vibration 2016;2016.
[65] Liu F, Zhou J. Research on fatigue strain and fatigue modulus of concrete. Advances in Civil Engineering 2017;2017.
[66] von der Haar C, Marx S. An additive strain model for fatigue-loaded concrete. BETON-UND STAHLBETONBAU 2017;112:31–40.
[67] von der Haar C, Marx S. A strain model for fatigue-loaded concrete. Structural Concrete 2018;19:463–71.
[68] Grünberg J, Göhlmann J, Marx S. Mechanische Modelle für mehraxiales Festigkeits- und Ermüdungsversagen von Stahlbeton. Beton-Und Stahlbetonbau 2014;109:403–16.
[69] Grünberg J, Göhlmann J. Schädigungsberechnung an einem Spannbetonschaft für eine Windenergieanlage unter mehrstufiger Ermüdung. Beton-Und Stahlbetonbau 2006;101:557–70.
[70] Pfanner D. Zur Degradation von Stahlbetonbauteilen unter Ermüdungsbeanspruchung. VDI-Verlag; 2003.
[71] Pfister T, Petryna Y, Stangenberg F. Damage modelling of reinforced concrete under multi-axial fatigue loading. Computational Modelling of Concrete Structures Balkema, Mayrhofen 2006:421–9.
[72] Oneschkow N. Fatigue behaviour of high-strength concrete with respect to strain and stiffness. International Journal of Fatigue 2016;87:38–49. https://doi.org/10.1016/j.ijfatigue.2016.01.008.
[73] Zanuy C, Albajar L, De la Fuente P. El proceso de fatiga del hormigón y su influencia estructural. Materiales de Construcción 2011:385–99.
[74] Alliche A. Damage model for fatigue loading of concrete. International Journal of Fatigue 2004;26:915–21.
[75] Desmorat R, Ragueneau F, Pham H. Continuum damage mechanics for hysteresis and fatigue of quasi-brittle materials and structures. International Journal for Numerical and Analytical Methods in Geomechanics 2007;31:307–29.
[76] Marigo JJ. Modelling of brittle and fatigue damage for elastic material by growth of microvoids. Engineering Fracture Mechanics 1985;21:861–74.

[77] Mai SH, Le-Corre F, Foret G, Nedjar B. A continuum damage modeling of quasi-static fatigue strength of plain concrete. International Journal of Fatigue 2012;37:79–85. https://doi.org/10.1016/j.ijfatigue.2011.10.006.
[78] Kindrachuk VM, Thiele M, Unger JF. Constitutive modeling of creep-fatigue interaction for normal strength concrete under compression. International Journal of Fatigue 2015;78:81–94.
[79] Kirane K, Bazant ZP. Enhanced microplane model for sub-critical crack growth and size effect under cyclic loading in isotropic quasibrittle solids. Int J Fatigue 2015;70:93–105.
[80] Caner FC, Bažant ZP, Wendner R. Microplane model M7f for fiber reinforced concrete. Engineering Fracture Mechanics 2013;105:41–57.
[81] Caner FC, Bažant ZP. Microplane model M7 for plain concrete. I: Formulation. Journal of Engineering Mechanics 2013;139:1714–23.
[82] Caner FC, Bažant ZP. Microplane Model M7 for Plain Concrete. II: Calibration and Verification. Journal of Engineering Mechanics 2013;139:1724–35. https://doi.org/10.1061/(ASCE)EM.1943-7889.0000571.
[83] Bažant Z, Gambarova P. CRACK SHEAR IN CONCRETE: CRACK BAND MICROPLANE MODEL 1984. https://doi.org/10.1061/(ASCE)0733-9445(1984)110:9(2015).
[84] Bažant ZP, Oh BH. Microplane model for progressive fracture of concrete and rock. Journal of Engineering Mechanics - ASCE 1985;111:559–82. https://doi.org/10.1061/(ASCE)0733-9399(1985)111:4(559).
[85] Bažant P, Oh BH. Efficient Numerical Integration on the Surface of a Sphere. ZAMM - Journal of Applied Mathematics and Mechanics / Zeitschrift Für Angewandte Mathematik Und Mechanik 1986;66:37–49. https://doi.org/10.1002/zamm.19860660108.
[86] Guo L-P, Carpinteri A, Roncella R, Spagnoli A, Sun W, Vantadori S. Fatigue damage of high performance concrete through a 2D mesoscopic lattice model. Computational Materials Science 2009;44:1098–106.
[87] Wang Y. Physical stochastic damage model for concrete subjected to fatigue loading. International Journal of Fatigue 2019;121:191–6.
[88] Zhaodong D, Jie L. A physically motivated model for fatigue damage of concrete. International Journal of Damage Mechanics 2018;27:1192–212.
[89] Cojocaru D, Karlsson AM. A simple numerical method of cycle jumps for cyclically loaded structures. International Journal of Fatigue 2006;28:1677–89.
[90] Eliáš J, Vořechovskỳ M, Skoček J, Bažant ZP. Stochastic discrete meso-scale simulations of concrete fracture: Comparison to experimental data. Engineering Fracture Mechanics 2015;135:1–16.
[91] Grassl P, Rempling R. A damage-plasticity interface approach to the meso-scale modelling of concrete subjected to cyclic compressive loading. Engineering Fracture Mechanics 2008;75:4804–18.
[92] Kandarpa S, Kirkner DJ, Spencer BF. Stochastic Damage Model for Brittle Materials Subjected to Monotonic Loading. Journal of Engineering Mechanics 1996;122:788–95. https://doi.org/10.1061/(ASCE)0733-9399(1996)122:8(788).
[93] Zheng SS, Tao QL, Liu B, Xie M, Hu Y. Study on Stochastic Damage Constitutive Relation for HSHPC Material Subjected to Uniaxial Tension Stress. Advanced Materials Research 2012;374–377:2570–3. https://doi.org/10.4028/www.scientific.net/AMR.374-377.2570.
[94] Eliáš J, Le J-L. Modeling of mode-I fatigue crack growth in quasibrittle structures under cyclic compression. Engineering Fracture Mechanics 2012;96:26–36.

[95] Van Mier JG. Concrete fracture: a multiscale approach. CRC press; 2012.
[96] Golewski GL. Physical characteristics of concrete, essential in design of fracture-resistant, dynamically loaded reinforced concrete structures. Material Design & Processing Communications 2019;1:e82. https://doi.org/10.1002/mdp2.82.
[97] Murdock JW. A critical review of research on fatigue of plain concrete. University of Illinois Bulletin; v 62, No 62 1965.
[98] Soerensen EV, Westhof L, Yde E, Serednicki A. Fatigue life of high performance grout for wind turbine grouted connection in wet or dry environment 2011:2.
[99] Rüsch H. Rüsch: Researches toward a general flexural theory... - Google Scholar 1960. https://scholar.google.com/scholar_lookup?title=Researches%20toward%20a%20general%20flexural%20theory%20for%20structural%20concrete&journal=Journal%20of%20the%20American%20Concrete%20Institute%2C%20Proc.&volume=57&issue=No.%201&pages=1-28&publication_year=1960&author=Rusch%2CH. (accessed August 26, 2021).
[100] Awad ME, Hilsdorf HK. STRENGTH AND DEFORMATION CHARACTERISTICS OF PLAIN CONCRETE SU BJECTED TO HIGH REP EATED AN D SUSTAINED lOADS 1971:298.
[101] Sparks PR, Menzies JB. The effect of rate of loading upon the static and fatigue strengths of plain concrete in compreSSI. on 1973:8.
[102] Cervo TC, Balbo JT. RESISTÊNCIA À FADIGA DE CONCRETOS CONVENCIONAIS PARA PAVIMENTAÇÃO 2004:12.
[103] Cornelissen, H.A.W. Fatigue Failure of Concrete in Tension. HERON, 29 (4), 1984 1984.
[104] Hanson JM, Somes MF, Helagson T. Investigation of Design Factors Affecting Fatigue Strength of Reinforcing Bars-Test Program. SP 1974;41:71–106. https://doi.org/10.14359/17678.
[105] Medeiros A, Zhang X, Ruiz G, Yu RC, Velasco M de SL. Effect of the loading frequency on the compressive fatigue behavior of plain and fiber reinforced concrete. International Journal of Fatigue 2015;70:342–50. https://doi.org/10.1016/j.ijfatigue.2014.08.005.
[106] Naik T, Singh S, Ye C. FATIGUE BEHAVIOR OF PLAIN CONCRETE MADE WITH OR WITHOUT FLY ASH 1993:1.
[107] Otto C, Elsmeier K, Lohaus L. Temperature Effects on the Fatigue Resistance of High-Strength-Concrete and High-Strength-Grout. In: Hordijk DA, Luković M, editors. High Tech Concrete: Where Technology and Engineering Meet, Cham: Springer International Publishing; 2018, p. 1401–9. https://doi.org/10.1007/978-3-319-59471-2_161.
[108] Raithby KD, Galloway JW. Effects of Moisture Condition Age, and Rate of Loading on Fatigue of Plain Concrete. SP 1974;41:15–35. https://doi.org/10.14359/17675.
[109] Tomann C, Lohaus L, Aldakheel F, Wriggers P. Influence of water-induced damage mechanisms on the fatigue deterioration of high-strength concrete. Proceedings of the 6th International Fib Congress: Concrete–Innovations in Materials, Design and Structures, Kraków, Poland, 2019, p. 27–9.
[110] Von der Haar C, Marx S. Strain Development of plain High Strength Concrete under Fatigue Loading. HiPerMat Ultra-High Perform Concr High Perform Constrution Mater 2016.
[111] Weigler H, Freitag W. DAUERSCHWELL-UND BETRIEBSFESTIGKEIT VON KONSTRUKTIONS-LEICHTBETON. Ernst; 1975.

[112] Zhang B, Phillips DV, Wu K. Effects of loading frequency and stress reversal on fatigue life of plain concrete. Magazine of Concrete Research 1996;48:361–75. https://doi.org/10.1680/macr.1996.48.177.361.
[113] Bažant ZP, Jirásek M. Creep and Hygrothermal Effects in Concrete Structures. Springer Netherlands; 2018. https://doi.org/10.1007/978-94-024-1138-6.
[114] Oneschkow N. Analyse des Ermüdungsverhaltens von Beton anhand der Dehnungsentwicklung. Berichte aus dem Institut für Baustoffe; 13 2014. https://doi.org/10.15488/357.
[115] Schneider S, Vöcker D, Marx S. Zum Einfluss der Belastungsfrequenz und der Spannungsgeschwindigkeit auf die Ermüdungsfestigkeit von Beton. Beton- und Stahlbetonbau 2012;107:836–45. https://doi.org/10.1002/best.201200054.
[116] Klausen D. FESTIGKEIT UND SCHAEDIGUNG VON BETON BEI HAEUFIG WIEDERHOLTER BEANSPRUCHUNG 1978.
[117] Cervo TC, Balbo JT. CALIBRAÇÃO DE FATOR LABORATÓRIO-CAMPO PARA PREVISÃO DE FADIGA DO CONCRETO EM PAVIMENTOS 2005:12.
[118] Thomas C, Sainz-Aja J, Setien J, Cimentada A, Polanco JA. Resonance fatigue testing on high-strength self-compacting concrete. Journal of Building Engineering 2021;35:102057.
[119] Nygard K, Petković G, Rosseland S, Stemland H. The influence of moisture conditions on the fatigue strength of concrete. Cement and Concrete Research Institute, SINTEF Report 1992.
[120] Muguruma H. Study on the low cycle fatigue behaviour of concrete members under submerged condition. Proceedings of the 26th Japan congress on materials research, 1983, p. 181–5.
[121] Muguruma H, Watanabe F. On the low-cycle compressive fatigue behaviour of concrete under submerged condition. Proceedings of the 27th Japan Congress on Materials Research, 1984, p. 219–24.
[122] Ohlsson U, Daerga PA, Elfgren L. Fracture energy and fatigue strength of unreinforced concrete beams at normal and low temperatures. Engineering Fracture Mechanics 1990;35:195–203.
[123] Mor A, Hester WT, Gerwick BC. Fatigue of High-Strength Reinforced Concrete. MJ 1992;89:197–207. https://doi.org/10.14359/2285.
[124] Miura T, Sato K, Nakamura H. Influence of primary cracks on static and fatigue compressive behavior of concrete under water. Construction and Building Materials 2021;305:124755. https://doi.org/10.1016/j.conbuildmat.2021.124755.
[125] Nakamura H, Nanri T, Miura T, Roy S. Experimental investigation of compressive strength and compressive fracture energy of longitudinally cracked concrete. Cement and Concrete Composites 2018;93:1–18.
[126] Bazant ZP, Schell WF. Fatigue Fracture of High-Strength Concrete and Size Effect. MJ 1993;90:472–8. https://doi.org/10.14359/3880.
[127] Grübl P, Weigler H, Karl S. Beton: Arten, Herstellung und Eigenschaften. John Wiley & Sons; 2002.
[128] Thiele M. Experimentelle Untersuchung und Analyse der Schädigungsevolution in Beton unter hochzyklischen Ermüdungsbeanspruchungen. PhD Thesis. Bundesanstalt für Materialforschung und-prüfung (BAM), 2016.
[129] Schneider S, Hümme J, Marx S, Lohaus L. Untersuchungen zum Einfluss der Probekörpergröße auf den Ermüdungswiderstand von hochfestem Beton. Beton- und Stahlbetonbau 2018;113:58–67. https://doi.org/10.1002/best.201700051.
[130] Hümme J. Ermüdungsverhalten von hochfestem Beton unter Wasser. Hannover: Institut für Baustoffe, Gottfried Wilhelm Leibniz Universität Hannover; 2018.

[131] Tepfers R, Görlin J, Samuelsson T. CONCRETE SUBJECTED TO PULSATING LOAD AND PULSATING DEFORMATION OF DIFFERENT PULSE WAVEFORM. Nordisk Betong 1973;17.
[132] Saini BS, Singh SP. Flexural fatigue strength prediction of self compacting concrete made with recycled concrete aggregates and blended cements. Construction and Building Materials 2020;264:120233.
[133] Golewski GL. An analysis of fracture toughness in concrete with fly ash addition, considering all models of cracking. IOP Conference Series: Materials Science and Engineering, vol. 416, IOP Publishing; 2018, p. 012029.
[134] Gil DM, Golewski GL. Effect of Silica Fume and Siliceous Fly Ash Addition on the Fracture Toughness of Plain Concrete in Mode I. IOP Conf Ser: Mater Sci Eng 2018;416:012065. https://doi.org/10.1088/1757-899X/416/1/012065.
[135] Vicente MA, González DC, Mínguez J, Tarifa MA, Ruiz G, Hindi R. Influence of the pore morphology of high strength concrete on its fatigue life. International Journal of Fatigue 2018;112:106–16. https://doi.org/10.1016/j.ijfatigue.2018.03.006.
[136] Morris AD, Garrett GG. A COMPARATIVE STUDY OF THE STATIC AND FATIGUE BEHAVIOUR OF PLAIN AND STEEL FIBRE REINFORCED MORTAR IN COMPRESSION AND DIRECT TENSION. International Journal of Cement Composites and Lightweight Concrete 1981;3.
[137] Yang F, Hu D, Zhou H, Teng M, Lan M, Teng Q. Post-fatigue properties of high-strength concrete subjected to coupled 3D fatigue-static loading. Construction and Building Materials 2021;306:124879. https://doi.org/10.1016/j.conbuildmat.2021.124879.
[138] Deutscher M, Tran NL, Scheerer S. Experimental Investigations on the Temperature Increase of Ultra-High Performance Concrete under Fatigue Loading. Applied Sciences 2019;9:4087. https://doi.org/10.3390/app9194087.
[139] Elsmeier K, Hümme J, Oneschkow N, Lohaus L. Prüftechnische Einflüsse auf das Ermüdungsverhalten hochfester feinkörniger Vergussbetone. Beton- und Stahlbetonbau 2016;111:233–40. https://doi.org/10.1002/best.201500065.
[140] Babadopulos LF de A, Sauzéat C, Di Benedetto H. Softening and local self-heating of bituminous mixtures during cyclic loading. Road Materials and Pavement Design 2017;18:164–77.
[141] Zhang B, Phillips DV, Wu K. Effects of loading frequency and stress reversal on fatigue life of plain concrete. Magazine of Concrete Research 1996;48:361–75. https://doi.org/10.1680/macr.1996.48.177.361.
[142] Vicente MA, González DC, Mínguez J, Tarifa MA, Ruiz G, Hindi R. Influence of the pore morphology of high strength concrete on its fatigue life. International Journal of Fatigue 2018;112:106–16. https://doi.org/10.1016/j.ijfatigue.2018.03.006.
[143] Myrtja E, Soudier J, Prat E, Chaouche M. Fatigue deterioration mechanisms of high-strength grout in compression. Construction and Building Materials 2021;270:121387. https://doi.org/10.1016/j.conbuildmat.2020.121387.